

Tree-Structure Expectation Propagation for LDPC Decoding over the BEC

Pablo M. Olmos, Juan José Murillo-Fuentes, and Fernando Pérez-Cruz

Abstract—We present the tree-structure expectation propagation (Tree-EP) to decode low-density parity-check (LDPC) codes over discrete memoryless channels (DMCs). EP generalizes belief propagation (BP) in two ways. First, it can be used with any exponential family distribution over the cliques in the graph. Second, it can impose additional constraints on the marginal distributions. We use this second property to impose pair-wise marginal constraints over pairs of variables connected to a check node of the LDPC code's Tanner graph. Thanks to these additional constraints, the Tree-EP marginal estimates for each variable in the graph are more accurate than those provided by BP. We also reformulate the Tree-EP algorithm for the binary erasure channel (BEC) as a peeling-type algorithm (TEP) and we show that the algorithm has the same computational complexity as BP and it decodes a higher fraction of errors. We describe the TEP decoding process by a set of differential equations that represents the expected residual graph evolution as a function of the code parameters. The solution of these equations is used to predict the TEP decoder performance in both the asymptotic regime and the finite-length regime over the BEC. While the TEP decoder asymptotically performs as the BP for regular and optimized codes. For finite-length LDPC codes, we derive a scaling law to predict the decoder performance that can be used for LDPC optimization.

I. INTRODUCTION

Low-density parity-check (LDPC) codes are well known channel capacity-approaching (c.a.) linear codes. In his PhD [1], Gallager proposed LDPC codes along with linear time practical decoding methods, among which the belief propagation (BP) algorithm plays a fundamental role. BP was later redescribed and popularized in the artificial intelligence community to perform approximate inference over graphical models, see for instance [2], [3], [4]. Given a factor graph that represents a joint probability density function (pdf) $p(\mathbf{V})$ of a set of discrete random variables [5], BP estimates the marginal probability function for each variable. It uses a local message passing algorithm between the nodes of the graph. The complexity of this algorithm is linear in the number of nodes [2]. For tree-like graphs, the BP solution is exact, but for graphs with cycles, BP is strictly suboptimal [6], [7], [8].

Linear block codes can be represented using factor (Tanner) graphs [9], where the factor nodes enforce the parity check

constraints. For LDPC codes, the presence of cycles in the Tanner graph quickly decays with the code length n . For large block lengths, a channel decoder based on BP achieves an excellent performance, close to the bitwise maximum a posteriori (bit-MAP) decoding, in certain scenarios [3], [10]. Nevertheless, the bit-MAP solution can only be achieved when the code length, code density and computational complexity go to infinity [11], [12].

The analysis of the BP for LDPC decoding over independent and identically distributed channels is detailed in [13], [14], in which the limiting performance and code optimization are addressed. For the binary erasure channel (BEC), the BP decoder presents an alternative formulation, in which the known variable nodes (encoded bits) are removed from the graph after each iteration. The BP, under this interpretation, is referred to as the *peeling decoder* (PD) [11]. In [15], the authors investigate the PD limiting performance by describing the expected LDPC graph evolution throughout the decoding process by a set of differential equations. The asymptotic performance for the BP decoder is summarized in the computation of the so-called *BP threshold* [10], [16], [11], [15], which defines the limit of the decodable region for an LDPC code.

The analysis of BP decoding performance in the finite-length regime is based on the evaluation of the presence of *stopping sets* (SSs) in the LDPC graph [13], which can severely degrade the decoder performance. In [13], [17], the authors provide tools to compute the exact BP average performance. However, this task becomes computationally challenging if the degree of irregularity or block length increases [11]. We can alternatively separate the contributions to the error rate of large-size errors, which dominate in the waterfall region [18], from small failures, which cause error floors [13]. On the one hand, *scaling laws* (SLs) were proposed in [18], [19] to accurately predict the BP performance in the waterfall region. For the BEC, they are based on the PD graph covariance evolution for a given graph as a function of the code length. Covariance evolution was solved for any LDPC ensemble in [20]. On the other hand, the analysis of the error floor is addressed by determining the dominant terms of the code weight distribution [13], [17]. Precise expressions for the asymptotic bit-MAP and BP error floor are derived in [1], [21], [22].

Expectation propagation (EP) [23] can be understood as a generalization of BP to construct tractable approximations of a joint pdf $p(\mathbf{V})$. Consider the set of all possible probability distributions in a given exponential family that map over the same factor graph. EP minimizes within this family the inclusive Kullback-Leibler (KL) divergence [24] with respect to $p(\mathbf{V})$. In [23], [25], it is shown that BP can be reformulated

This work was partially funded by Spanish government (Ministerio de Educación y Ciencia, TEC2009-14504-C02-01,02, Consolider-Ingenio 2010 CSD2008-00010), Universidad Carlos III (CCG10-UC3M/TIC-5304) and European Union (FEDER).

P. M. Olmos and J.J. Murillo-Fuentes are with the Dept. Teoría de la Señal y Comunicaciones, Escuela Técnica Superior de Ingeniería, Universidad de Sevilla, Paseo de los Descubrimientos s/n, 41092 Sevilla, Spain. E-mail: {olmos, murillo}@us.es

F. Pérez-Cruz is with Dept. Teoría de la Señal y Comunicaciones, Universidad Carlos III de Madrid (Spain). E-mail: fernando@tsc.uc3m.es

as EP by considering a discrete family of pdfs that factorizes as the product of single-variable multinomial terms, i.e. $q(\mathbf{V}) = q_1(V_1)q_2(V_2)\dots q_n(V_n)$. EP generalizes BP in two ways: first, it is not restricted to discrete random variables. And second, EP naturally formulates to include more versatile approximating factorizations [26], [27]. In this paper, we focus on EP to construct a Markov tree-structure to approximate the original graph. Conditional factors in the tree-structure are able to capture pairwise interactions that single factors neglect. We refer to this algorithm as *tree-structured expectation propagation* (Tree-EP). We borrow from the theoretical framework of the Tree-EP algorithm to design a new decoding approach to decode LDPC codes over the discrete memoryless channels (DMCs). Then we analyze in detail the decoder performance for the BEC.

For erasure channels, we show that the Tree-EP can be reinterpreted as a peeling-type algorithm that formulates as an improved PD. We refer to this simplified algorithm as the TEP decoder. The TEP decoder was presented in [28], [29], where we empirically observed a noticeable gain in performance compared to BP for both regular and irregular LDPC codes. We explain, analyze and predict this gain in performance for any LDPC code. First, we extend to the TEP decoder the methodology proposed in [15] to evaluate the expected graph evolution of the LDPC's Tanner graph in the asymptotic case. As the block sizes increases, we show the conditions for which the TEP decoder could improve the BP decoder. Nevertheless, for typical LDPC ensembles the TEP decoder is not able to improve the BP solution. In the second part of the paper, we concentrate on practical finite-length codes and we explain the gain provided by the TEP decoder compared to BP. Furthermore, we derive an SL that accurately predicts the performance for any given LDPC ensemble in the waterfall region. This SL can be used for TEP-oriented finite-length optimization. Finally, we also prove that the decoder complexity is of the same order than BP, i.e. linear in the number of variables, unlike other techniques proposed to improve BP at a higher computational cost. For instance, we can mention variable guessing algorithms [30], the Maxwell decoder [12] and pivoting algorithms for efficient Gaussian elimination [31], [32], [33].

The rest of the paper is organized as follows. Section II is devoted to introducing the Tree-EP algorithm for block decoding over DMCs. In Section III, we particularize the algorithm for the BEC, yielding the TEP decoder and we analyze its properties. In Section IV, we derive the differential equations that describe the decoder behavior for a given LDPC graph and we investigate the asymptotic behavior. In Section V, we propose an scaling law to predict the TEP finite-length performance for a given LDPC ensemble in the waterfall region. We conclude the paper in Section VI.

II. TREE-EP FOR LDPC DECODING LDPC OVER MEMORYLESS CHANNELS

Consider an LDPC binary code \mathcal{C} with parity check matrix \mathbf{H} , of dimensions $k \times n$, where $k = n(1 - r)$, n is the code length and r the rate of the code. By definition, any vector

\mathbf{v} in \mathbb{F}_2^n belongs to the code \mathcal{C} as long as $\mathbf{v}\mathbf{H}^\top = \mathbf{0}$, where \mathbb{F}_2^n is the n -dimensional binary Galois field. Each row of \mathbf{H} therefore imposes a zero parity linear restriction between a subset of variables:

$$\mathcal{C}_j(\mathbf{v}) \doteq \mathbb{1} \left[\sum_{i \in I_j} v_i \bmod 2 = 0 \right] \quad \forall j = 1, \dots, k, \quad (1)$$

where v_i is the i -th component of \mathbf{v} , I_j is the set of positions where the j -th row of \mathbf{H} is one and $\mathbb{1}[\cdot]$ is a boolean operator, which takes value one if the condition in its argument is verified. Note that, given the definition in (1), we can write $\mathbb{1}[\mathbf{v} \in \mathcal{C}] = \mathcal{C}_1(\mathbf{v})\mathcal{C}_2(\mathbf{v})\dots\mathcal{C}_k(\mathbf{v})$.

Assume that an unknown codeword is transmitted through a discrete memoryless channel [24] and let $\mathbf{y} \in \mathcal{A}(\mathbf{y})$ be the observed channel output, where $\mathcal{A}(\mathbf{y})$ is the channel output alphabet. A bit-MAP decoder [34] minimizes the bit error rate (BER) by estimating the transmitted vector $\hat{\mathbf{v}} = [\hat{v}_1, \hat{v}_2, \dots, \hat{v}_n]$ as follows¹:

$$\begin{aligned} \hat{v}_u &= \arg \max_{v \in \{0,1\}} p(V_u = v | \mathbf{y}) = \arg \max_{v \in \{0,1\}} \sum_{\mathbf{V} \in \mathcal{C}: V_u = v} p(\mathbf{V} | \mathbf{y}) \\ &= \arg \max_{v \in \{0,1\}} \sum_{\mathbf{V} \in \mathcal{C}: V_u = v} p(\mathbf{y} | \mathbf{V}) p(\mathbf{V}) \\ &= \arg \max_{v \in \{0,1\}} \sum_{\mathbf{V}: V_u = v} \prod_{i=1}^n p(y_i | V_i) \prod_{j=1}^k \mathcal{C}_j(\mathbf{V}) \end{aligned} \quad (2)$$

for $u = 1, \dots, n$, where we have assumed that the channel is memoryless and that all codewords are equally probable

$$p(\mathbf{V}) = \frac{\mathbb{1}[\mathbf{V} \in \mathcal{C}]}{2^{nr}}. \quad (3)$$

For most LDPC codes of interest, the factor graph [35] associated to the product $p(\mathbf{y} | \mathbf{V}) p(\mathbf{V})$ in (2) yields a graph with cycles [36]. Hence, the exact computation of the marginals $p(V_u = v | \mathbf{y})$ grows exponentially with the number of coded bits [6]. Belief propagation [1], [2], [3] is nowadays the standard algorithm to efficiently solve this problem in coding applications, because accurate estimates for each marginal are obtained at linear cost with n . Besides, BP can be cast as an approximation of $p(\mathbf{V} | \mathbf{y})$ in (2) by a complete disconnected factor graph, i.e.

$$p(\mathbf{V} | \mathbf{y}) \propto \prod_{i=1}^n p(y_i | V_i) \prod_{j=1}^k \mathcal{C}_j(\mathbf{V}) \approx \prod_{i=1}^n \hat{q}_{i,\text{BP}}(V_i), \quad (4)$$

where $\hat{q}_{i,\text{BP}}(V_i)$ is the BP estimate for the i -th variable [6], [37], [38].

A. Tree-EP algorithm for LDPC decoding

The Tree-EP algorithm [26], [39] improves BP decoding because it approximates the posterior $p(\mathbf{V} | \mathbf{y})$ in (2) with a tree (or forest) Markov-structure between the variables, i.e.:

$$q(\mathbf{V}) = \prod_{i=1}^n q_i(V_i | V_{p_i}), \quad (5)$$

¹In the following, we use lower case letters to denote a particular realization of a random variable or vector, e.g. $\mathbf{V} = \mathbf{v}$ means that \mathbf{V} takes the \mathbf{v} value.

where the set of pairs $\{(i, p_i)_{i=1}^n\}$ forms a tree graph over the original set of variables nodes and $q_i(V_i|V_{p_i})$ approximates the conditional probability $p(V_i|V_{p_i}, \mathbf{y})$. For some variable nodes V_{p_i} might be missing, i.e. p_i is empty, and we use single-variable factors $q_i(V_i)$ to approximate them.

Using the approximation in (5), the complexity of the marginalization in (2) is linear with the number of variables. In [39], it is shown that the approximation in (5) provides more accurate estimates for the marginals $p(V_u|\mathbf{y})$ in (2) than BP, since it captures information about the joint marginal of pairs of variables that are then propagated through the graph. Indeed, note that the factorization in (4) is just a particular case of (5), because EP converges to the same solution as the BP [23], [25], when we consider a completely disconnected graph, i.e. $p_i = \emptyset \forall i$.

Consider a family of discrete probability distributions that factorize according to (5), denoted hereafter by \mathcal{F}_{tree} . The optimal choice for $q(\mathbf{V}) \in \mathcal{F}_{tree}$, denoted by $\hat{q}(\mathbf{V})$, is such that it minimizes the inclusive KL divergence² with $p(\mathbf{V}|\mathbf{y})$:

$$\hat{q}(\mathbf{V}) = \arg \min_{q(\mathbf{V}) \in \mathcal{F}_{tree}} D_{KL}(p(\mathbf{V}|\mathbf{y})||q(\mathbf{V})). \quad (6)$$

The next lemma, first proved in [40], states that the resolution of the problem in (6) is as complex as the bit-MAP decoding problem in (2). In both cases we have to perform exact marginalization over the posterior distribution $p(\mathbf{V}|\mathbf{y})$.

Lemma 1: (Moment matching for inclusive KL-divergence minimization). Consider a set of discrete random variables \mathbf{V} with joint pdf $p(\mathbf{V})$. Let \mathcal{F}_* be a family of probability distributions that share a common generic factorization:

$$q(\mathbf{V}) \in \mathcal{F}_* \Leftrightarrow q(\mathbf{V}) = \prod_{i=1}^L q_i(\mathbf{V}_i), \quad (7)$$

for some normalized functions $q_i(\mathbf{V}_i)$, where \mathbf{V}_i is a subset of \mathbf{V} , for $i = 1, \dots, L$. Under these conditions, the function $\hat{q}(\mathbf{V})$ in \mathcal{F}_* such that

$$\hat{q}(\mathbf{V}) = \arg \min_{q(\mathbf{V}) \in \mathcal{F}_*} D_{KL}(p(\mathbf{V})||q(\mathbf{V})) \quad (8)$$

is constructed as follows:

$$\hat{q}_i(\mathbf{V}_i) = \sum_{\mathbf{V} \sim \mathbf{V}_i} p(\mathbf{V}), \quad i = 1, \dots, L \quad (9)$$

$$\hat{q}(\mathbf{V}) = \prod_{i=1}^L \hat{q}_i(\mathbf{V}_i), \quad (10)$$

where $\mathbf{V} \sim \mathbf{V}_i$ denotes all the variables in \mathbf{V} except those in \mathbf{V}_i .

Proof: The proof of this lemma can be found in [40], [41]. ■

²We refer to the inclusive KL divergence when we minimize $D_{KL}(p||q)$ and to the exclusive KL divergence when we minimize $D_{KL}(q||p)$, which is the one used for mean-field approximations, see [39] for a discussion.

Lemma 1 can be directly applied to the problem in (6) and the optimum Markov-tree $\hat{q}(\mathbf{V})$ is such that

$$\hat{q}_i(V_i|V_{p_i}) = \frac{\sum_{\mathbf{V} \sim \{V_i, V_{p_i}\}} p(\mathbf{V}|\mathbf{y})}{\sum_{\mathbf{V} \sim V_{p_i}} p(\mathbf{V}|\mathbf{y})} = p(V_i|V_{p_i}, \mathbf{y}) \quad (11)$$

for $i = 1, \dots, n$ and

$$\hat{q}(\mathbf{V}) = \prod_{i=1}^n \hat{q}_i(V_i|V_{p_i}). \quad (12)$$

The marginal computation in (11) is of the same complexity order as (2).

The Tree-EP algorithm overcomes this problem by iteratively approaching $\hat{q}(\mathbf{V})$. Define $q^\ell(\mathbf{V})$ as the TEP approximation to $\hat{q}(\mathbf{V})$ at the end of the ℓ -th iteration and let $q^\infty(\mathbf{V}) \approx \hat{q}(\mathbf{V})$ be the Tree-EP solution after convergence³. Let $w_{z,j}^\ell(V_z, V_{p_z})$ be non-negative real functions, with $z = 1, \dots, n$ and $j = 1, \dots, k$, that are updated at each iteration so that

$$W_j^\ell(\mathbf{V}) = \prod_{z=1}^n w_{z,j}^\ell(V_z, V_{p_z}), \quad (13)$$

is the approximation to the parity function $C_j(\mathbf{V})$ at iteration ℓ . Thus, the Tree-EP approximation to the posterior $p(\mathbf{V}|\mathbf{y})$ at iteration ℓ , i.e $q^\ell(\mathbf{V})$, is constructed as follows:

$$\begin{aligned} q^\ell(\mathbf{V}) &= \prod_{z=1}^n q_z^\ell(V_z|V_{p_z}) \\ &\doteq \prod_{z=1}^n p(y_z|V_z) \prod_{j=1}^k W_j^\ell(\mathbf{V}) \\ &= \prod_{z=1}^n \left(p(y_z|V_z) \prod_{j=1}^k w_{z,j}^\ell(V_z, V_{p_z}) \right). \end{aligned} \quad (14)$$

The Tree-EP is described in detail in Algorithm 1. At iteration ℓ , only the m -th factor, $W_m^\ell(\mathbf{V})$, is refined. In Step 7 we replace $W_m^{\ell-1}(\mathbf{V})$ by the true value $C_m(\mathbf{V})$ in the $q^{\ell-1}(\mathbf{V})$ function. The resulting function is denoted by $f(\mathbf{V}, \ell, m)$. Then, by Lemma 1, in Steps 8 to 10 we compute $q^\ell(\mathbf{V})$ as the solution of the following problem

$$q^\ell(\mathbf{V}) = \arg \min_{q(\mathbf{V}) \in \mathcal{F}_{tree}} D_{KL}(f(\mathbf{V}, \ell, m)||q(\mathbf{V})). \quad (15)$$

At this point, the TEP solution becomes suboptimal with respect to (6) but tractable: the computation of the marginals $q(V_i|V_{p_i})$ for $i = 1, \dots, n$ over $f(\mathbf{V}, \ell, m)$ in (20) and (21) can be performed efficiently. Let us first express the factorization

³EP as BP might not converge for loopy graphs [39].

of $f(\mathbf{V}, \ell, m)$ in a more convenient way:

$$\begin{aligned} f(\mathbf{V}, \ell, m) &= \mathbf{C}_m(\mathbf{V}) \frac{q^{\ell-1}(\mathbf{V})}{W_m^{\ell-1}(\mathbf{V})} \\ &= \mathbf{C}_m(\mathbf{V}) \prod_{z=1}^n p(y_z | V_z) \prod_{\substack{j=1 \\ j \neq m}}^k W_j^{\ell-1}(\mathbf{V}) \\ &= \mathbf{C}_m(\mathbf{V}) \prod_{z=1}^n g_z^{\ell-1, m}(V_z, V_{p_z}), \end{aligned} \quad (16)$$

where we have introduced the following auxiliary functions

$$g_z^{\ell-1, m}(V_z, V_{p_z}) \doteq p(y_z | V_z) \prod_{\substack{j=1 \\ j \neq m}}^k w_{z,j}^{\ell-1}(V_z, V_{p_z}). \quad (17)$$

Therefore, the marginalization of (16) in (20) yields

$$q(V_i, V_{p_i}) = \sum_{\mathbf{V} \sim \{V_i, V_{p_i}\}} \mathbf{C}_m(\mathbf{V}) \prod_{z=1}^n g_z^{\ell-1, m}(V_z, V_{p_z}). \quad (18)$$

As in (13), the product $\prod_{z=1}^n g_z^{\ell-1, m}(V_z, V_{p_z})$ maps over the same factor graph than the tree structure chosen in (5). Therefore, the presence of cycles in the factor graph of $f(\mathbf{V}, \ell, m)$ is due to the parity factor $\mathbf{C}_m(\mathbf{V})$. The graph is cycle-free as long as, among the variables connected to the parity check node $\mathbf{C}_m(\mathbf{V})$, none of them are linked by a conditional term $q(V_i | V_{p_i})$ in (5), as illustrated in Fig. 1(a). Otherwise the graph presents cycles, as shown in Fig. 1(b). In the first case, the marginal computation in (20) is solved at linear cost by message passing. For the latter, where the graph is not completely cycle-free, we can compute the pairwise marginals using Pearl's cutset conditioning algorithm [26], [42]. These cycles play a crucial role in understanding why the Tree-EP algorithm outperforms the BP solution.

Pearl's algorithm proceeds by breaking each cycle assuming a set of the variables involved as known, e.g. V_o in Fig. 1(b). Then, the marginals of the remaining variables can be computed at low-cost by message passing. The overall complexity of this method is exponential with the number of assume-observed variables. However, we prove that for the BEC the complexity of the Tree-EP algorithm is linear with the number of variables, i.e. of the same order as BP. If a completely disconnected approximation is considered, i.e. $q(\mathbf{V}) = \prod_i q_i(V_i)$, $f(\mathbf{V}, \ell, m)$ is always cycle free and each Tree-EP iteration is performed at linear complexity with n . Since this case is equivalent to BP [23], [25], the EP algorithm with a disconnected approximation is identical to BP.

III. TREE-EP DECODING FOR THE BEC

For the BEC, the likelihood function for a particular variable V_i , $p(y_i | V_i)$, provides a complete description about its value when it has not been erased:

$$p(y_i = 1 | V_i = 1) = 1 - \epsilon, \quad p(y_i = 1 | V_i = 0) = 0, \quad (23)$$

$$p(y_i = 0 | V_i = 1) = 0, \quad p(y_i = 0 | V_i = 0) = 1 - \epsilon. \quad (24)$$

In this case, we say that the variable is known. Otherwise, when the variable is erased, the likelihood function for this

Algorithm 1 Tree-EP algorithm for a predefined tree structure.

- 1: $\ell = 0$.
- 2: Initialize $W_j^0(\mathbf{V}) = 1$ for $j = 1, \dots, k$.
- 3: Initialize $q^0(\mathbf{V}) = \prod_{i=1}^n p(y_i | V_i)$.
- 4: **repeat**
- 5: $\ell = \ell + 1$.
- 6: Chose a $W_m^\ell(\mathbf{V})$ to refine: $m = \text{mod}(\ell, k)$.
- 7: Remove $W_m^{\ell-1}(\mathbf{V})$ from $q^{\ell-1}(\mathbf{V})$ and include the *true term* $\mathbf{C}_m(\mathbf{V})$:

$$f(\mathbf{V}, \ell, m) \doteq \mathbf{C}_m(\mathbf{V}) \frac{q^{\ell-1}(\mathbf{V})}{W_m^{\ell-1}(\mathbf{V})}. \quad (19)$$

- 8: Compute $q_i^\ell(V_i, V_{p_i})$ and $q_i^\ell(V_i)$ for $i = 1, \dots, n$:

$$q_i^\ell(V_i, V_{p_i}) \propto \sum_{\mathbf{V} \sim \{V_i, V_{p_i}\}} f(\mathbf{V}, \ell, m), \quad (20)$$

$$q_i^\ell(V_i) = \sum_{V_{p_i}} q_i^\ell(V_i, V_{p_i}). \quad (21)$$

- 9: Compute $q_i^\ell(V_i | V_{p_i}) = \frac{q_i^\ell(V_i, V_{p_i})}{q_i^\ell(V_{p_i})}$ for $i = 1, \dots, n$.

- 10: $q^\ell(\mathbf{V}) = \prod_{i=1}^n q_i^\ell(V_i | V_{p_i})$.

- 11: Compute $w_{i,m}^\ell(V_i, V_{p_i})$ from $q^\ell(\mathbf{V})$. By (14),

$$w_{i,m}^\ell(V_i, V_{p_i}) = \frac{q_i^\ell(V_i | V_{p_i})}{p(y_i | V_i) \prod_{\substack{j=1 \\ j \neq m}}^k w_{i,j}^{\ell-1}(V_i, V_{p_i})} \quad (22)$$

for $i = 1, \dots, n$.

- 12: $W_m^\ell(\mathbf{V}) = \prod_{i=1}^n w_{i,m}^\ell(V_i, V_{p_i})$.

- 13: **until** all $W_j^\ell(\mathbf{V})$, $j = 1, \dots, k$, converge.

- 14: $\hat{q}(\mathbf{V}) \approx q^\infty(\mathbf{V})$.
-

variable is constant and the uncertainty about its value is complete:

$$p(y_i = ? | V_i = 1) = p(y_i = ? | V_i = 0) = \epsilon. \quad (25)$$

This two-state behavior of the likelihood function makes the pairwise marginal functions $q_i^\ell(V_i, V_{p_i})$ in (18) and (20) alternate between just four states, depending on what we know about these variables at the end of the ℓ -th iteration. Furthermore, we can describe a finite set of scenarios for which $q_i^\ell(V_i, V_{p_i})$ might alternate between these states. This result is used later to propose a simplified reformulation of the decoding algorithm. Let us detail the possible outcomes and cases of interest by running the algorithm at different times.

Iteration $\ell = 1$. In Step 7, we compute

$$f(\mathbf{V}, \ell = 1, m = 1) = \mathbf{C}_1(\mathbf{V}) \prod_{z=1}^n p(y_z | V_z), \quad (26)$$

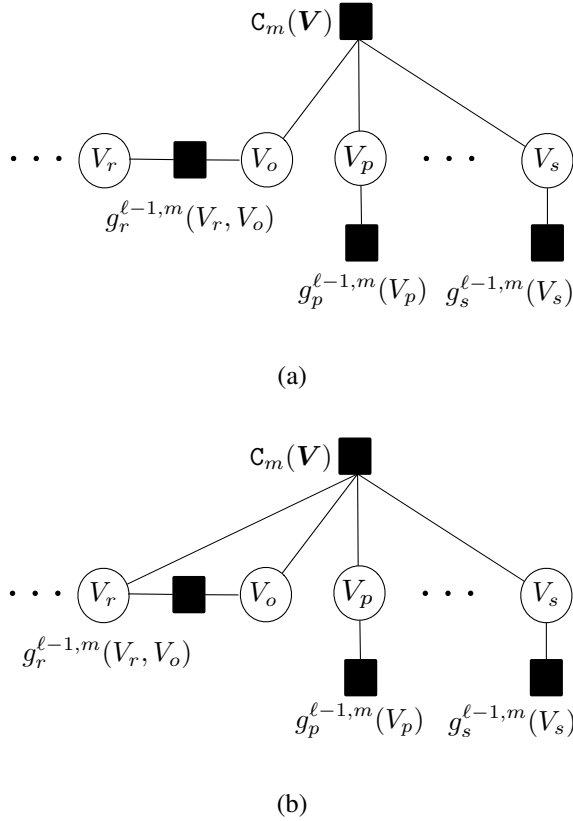


Fig. 1. Example of factor graph associated to $f(\mathbf{V}, \ell, m)$. In (a), the graph is cycle free since C_m does not connect any variable V_i with its parent V_{p_i} . In (b), the graph has a cycle since both V_r and $V_{p_r} = V_o$ belong to I_m .

where the likelihood terms $p(y_z|V_z)$ for $z = 1, \dots, n$ take the form (23)-(25). Over (26), we compute the marginals of $\{(V_i, V_{p_i})_{i=1}^n\}$. For any pair (V_i, V_{p_i}) , we observe the following scenarios:

- If V_i and V_{p_i} have not been erased, then marginalization yields:

$$q_i^1(V_i, V_{p_i}) \propto p(y_i|V_i)p(y_{p_i}|V_{p_i}) = \mathbb{1}[V_i = v_1, V_{p_i} = v_2], \quad (27)$$

where v_1 and v_2 are, respectively, the values of V_i and V_{p_i} .

- If V_i is erased and V_{p_i} is not, then the marginalization in (26) might reveal the value of V_i . This scenario only happens if V_i is connected to the check $C_1(\mathbf{V})$ and, in addition, the rest of variables connected to this check are known. In this way, the parity restriction fixes the value of the variable and the marginalization yields the same result than in (27). Otherwise V_i remains unknown:

$$q_i^1(V_i, V_{p_i}) = \frac{1}{2} \mathbb{1}[V_{p_i} = v_2], \quad (28)$$

where v_2 is the value of V_{p_i} . For instance, assume that, in Fig. 1 (a), V_o and V_p are known. When we compute the marginal for V_s , this variable gets revealed.

- The case where V_{p_i} is erased and V_i is not is symmetric to the previous scenario.

- If both V_i and V_{p_i} are erased, we compute

$$q_i^1(V_i, V_{p_i}) \propto \sum_{\mathbf{V} \sim \{V_i, V_{p_i}\}} C_m(\mathbf{V}) \prod_{\substack{z=1 \\ z \neq \{i, p_i\}}}^n p(y_z|V_z) = 1/4 \quad (29)$$

for any (V_i, V_{p_i}) pair unless these two variables are the only unknown variables connected to the check $C_m(\mathbf{V})$. In this case, due to the parity constraint, only one value of $V_i + V_{p_i}$ makes $q_i^1(V_i, V_{p_i})$ non-zero. In other words, an equality or inequality relationship between both variables is found and $q_i^1(V_i, V_{p_i})$ either takes the form of

$$q_i^1(V_i, V_{p_i}) = \frac{1}{2} \mathbb{1}[V_i = V_{p_i}] \quad (30)$$

or

$$q_i^1(V_i, V_{p_i}) = \frac{1}{2} \mathbb{1}[V_i \neq V_{p_i}]. \quad (31)$$

For instance, assume that, in Fig. 1(b), V_p and V_s are known. Then, we learn that V_r is equal or opposite to V_o .

The latter is of importance to explain the advantage of the TEP decoder over BP, because we only obtain the result in (30) or (31) if we compute pairwise marginals. The BP algorithm uses only a disconnected approximation for the factors (4) and from them we cannot derive the (in)equality constraints in (30) and (31).

It can be readily check for the BEC that when we compute the functions $q_i^\ell(V_i|V_{p_i})$ and $w_{i,m}^\ell(V_i, V_{p_i})$ in Steps 9, 10 and 11 of the algorithm, they are proportional to the pairwise marginal computed above⁴:

$$q_i^\ell(V_i|V_{p_i}) \propto q_i^\ell(V_i, V_{p_i}), \quad (34)$$

$$w_{i,m}^\ell(V_i, V_{p_i}) \propto q_i^\ell(V_i, V_{p_i}). \quad (35)$$

Iteration ℓ . We follow a induction procedure to analyze the result of the ℓ -th iteration. Given the factorization of the function $f(\mathbf{V}, \ell, m)$ in (16), the current information of each variable is contained in the $g_z^{\ell-1,m}(V_z, V_{p_z})$ functions for $z = 1, \dots, n$ in (17). By crossing (35) and (17), we observe that these functions are also proportional to $q_z^{\ell-1}(V_z, V_{p_z})$. Therefore,

$$f(\mathbf{V}, \ell, m) \propto C_m(\mathbf{V}) \prod_{z=1}^n q_z^{\ell-1}(V_z, V_{p_z}). \quad (36)$$

By enumerating the possible outcomes of the marginal $q_i^\ell(V_i, V_{p_i})$ over $f(\mathbf{V}, \ell, m)$ in (36), we conclude that the discussion for $\ell = 1$ extends for this case almost literally. By induction, we have proved that the functions $q_i^\ell(V_i, V_{p_i})$ only belong to one of the four states described in (27)-(31).

⁴For instance, if we assume that $q_i^\ell(V_i, V_{p_i})$ is of the form of (27), we first compute $q(V_{p_i})$:

$$q(V_{p_i}) = \sum_{V_i} q(V_i, V_{p_i}) = \mathbb{1}[V_{p_i} = v_1] \quad (32)$$

and, therefore,

$$q_i^\ell(V_i|V_{p_i}) = \frac{\mathbb{1}[V_i = v_1, V_{p_i} = v_2]}{\mathbb{1}[V_{p_i} = v_1]} = \mathbb{1}[V_i = v_1, V_{p_i} = v_2], \quad (33)$$

where we take $q_i^\ell(V_i|V_{p_i}) = 0$ when $q(V_{p_i}) = 0$.

Nevertheless, for any $\ell > 1$, we reveal a new scenario for which a variable can be de-erased, thanks to the imposed (in)equality pairwise condition in (30) and (31). Assume that at iteration $\ell - 1$, we learn that V_r and V_o are equal and at iteration ℓ we process the check node $C_m(\mathbf{V})$ depicted Fig. 1 (b). If $V_s = 0$, then the erased variable V_p should be zero to fulfill the parity constraint. This scenario is not possible if we cannot capture equality relationships, which are void for the BP decoder. Therefore, the tree structured approximation in (5) provides with respect to the BP procedure an extra case in which a variable can be de-erased. The key aspect is to find equality conditions between variables that can be used to decode other variables related to them by parity functions.

The Tree-EP procedure for BEC can be cast as the sequential search of three particular scenarios to perform the inference, where the only thing that matters is the number of unrevealed variables in the processed check node. We can further simplify and reformulate this procedure as a peeling-type decoder. The key idea is to simplify the LDPC Tanner graph according to the information that we sequentially obtain from the encoded bits. We rename this reformulated algorithm as the TEP decoder [28], [29].

A. The TEP decoder

Before detailing the TEP decoder algorithm, let us introduce some basic definitions about Tanner graphs. The Tanner graph of an LDPC code is induced by the parity-check matrix \mathbf{H} as described in [9], [34]. The graph has n variable nodes V_1, \dots, V_n and $k = n(1 - r)$ parity check nodes P_1, \dots, P_k . The degree of a check node, denoted as d_{P_j} , is the number of variable nodes connected to it in the graph. Similarly, the degree of a variable node, denoted as d_{V_i} , is the number of check nodes connected to that variable node. In the Tanner graph, we associate a zero parity value to each check node in the graph. As we iterate, the parity of a certain check node P_j , which is denoted hereafter as $[P_j]$, might change.

The TEP decoder is detailed in Algorithm 2. It is based on the sequential procedure of degree-one and two check nodes in the graph. Processing a degree-one check node in Steps 10-12 of Algorithm 2 is equivalent to find an erased variable connected to a check node where the rest of variables are known. Since the BP solution is restricted to this case, the description of the BP as a peeling-type algorithm is obtained if we do not consider Steps 13-16 in Algorithm 2 [15], [43]. In this sense, the TEP decoder emerges as an improved PD. Besides, we claim that the complexity of both decoders is of the same order, i.e. $\mathcal{O}(n)$. We intentionally leave to Section III-B a detailed analysis of the TEP complexity.

The removal of a degree-two check node in Steps 13-16 of Algorithm 2 represents the inference of an equality or inequality relationship. This process is sketched in Fig. 2. The variable V_1 heirs the connections of V_2 (solid lines) in Fig. 2(b). Finally, the check P_1 and the variable V_2 can be removed, as shown in Fig. 2(c), because they have no further implication in the decoding process. V_2 is de-erased once V_1 is de-erased. Note that, when we remove a check node of degree two, we usually create a variable node with a higher degree while the degree of the check nodes remain unaltered.

Algorithm 2 TEP algorithm for LDPC decoding over BEC.

- 1: Let \mathbf{y} be the received codeword: $\mathbf{y} \in \{0, ?, 1\}^n$.
 - 2: Construct the index set $\bar{\xi} : \forall s \in \bar{\xi}$ then $y_s \neq ?$.
 - 3: **for all** $s \in \bar{\xi}$ **do**
 - 4: Remove from the graph variable node V_s .
 - 5: If $y_s = 1$, flip the parity of the check nodes connected to V_s .
 - 6: **end for**
 - 7: **repeat**
 - 8: Look for a check node of degree one or two.
 - 9: **if** P_j is found with degree one, connected to V_s , **then**
 - 10: V_s is decoded with value $[P_j]$.
 - 11: Remove both V_s and P_j from the graph.
 - 12: If $[P_j] = 1$, flip the parity of the check nodes connected to V_s .
 - 13: **else if** P_j is found with degree two, connected to V_o and V_r , **then**
 - 14: Remove P_j and V_o from the graph.
 - 15: If $[P_j] = 1$, flip the parity of the check nodes connected to V_o .
 - 16: Reconnect to V_r the check nodes connected to V_o .
 - 17: **end if**
 - 18: **until** the graph is empty or there are no degree-one or two check nodes in the graph
-

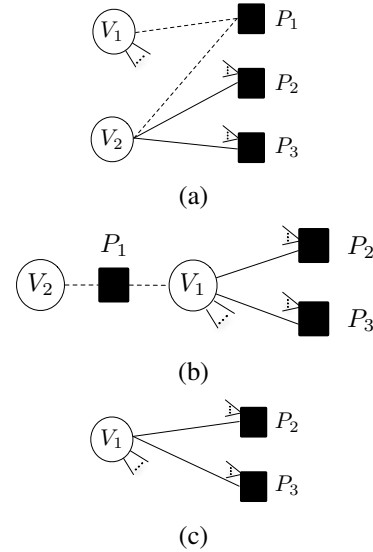


Fig. 2. In (a) we show two variable nodes, V_1 and V_2 , that share a check node of degree two, P_1 . In (b), V_1 heirs the connections of V_2 (solid lines). In (c), we show the graph once P_1 and V_2 have been removed. If P_1 is parity one, the parities of P_2 , P_3 are reversed.

The TEP decoder eventually creates additional check nodes of degree one when we find a scenario equivalent to the one depicted in Fig. 3. Consider two variable nodes connected to a check node of degree two that also share another check node with degree three, as illustrated in Fig. 3(a). After removing the check node P_3 and the variable node V_2 , the check node

P_4 is now degree one, as illustrated in Fig. 3(b). At the beginning of the decoding algorithm, this scenario is very unlikely. However, as we remove variable and check nodes, the probability of this event grows, as we are reducing the graph and increasing the degree of the remaining variable nodes.

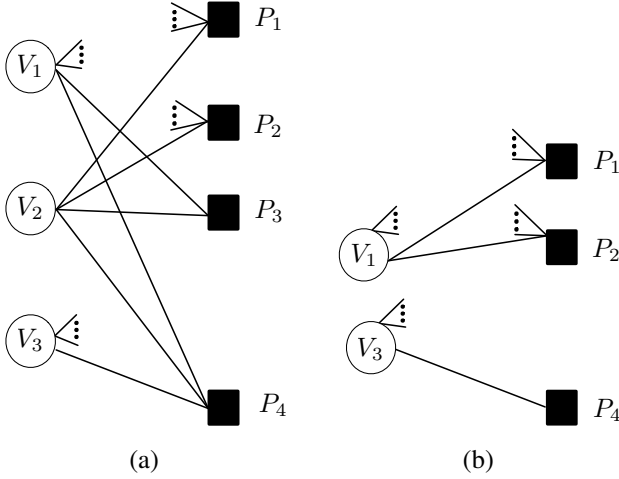


Fig. 3. In (a), the variables V_1 and V_2 are connected to a two-degree check node, P_3 , and they also share a check node of degree three, P_4 . In (b) we show the graph once the TEP has removed P_3 and V_2 .

Another important result of the TEP algorithm is that it applies the Tree-EP algorithm with no initial pairwise relations. The tree structure is not fixed a priori. It dynamically includes a new pairwise relation in the tree structure whenever it processes a degree-two check node. In Appendix A, we show that the TEP decoding is independent of the ordering in which the variables are processed, as different processing orderings yield equivalent trees in the graph.

B. TEP decoder complexity

In the next two lemmas we prove that, for LDPC codes, the TEP complexity linearly scales with the code length n :

Lemma 2: Consider a transmission over a BEC of parameter ϵ using an LDPC code \mathcal{C} where variable and check nodes degrees are bounded, and code length $n \rightarrow \infty$. Let $\Lambda_{\text{avg}}(t, \mathbf{y}, \mathcal{C})$ and $\Theta_{\text{avg}}(t, \mathbf{y}, \mathcal{C})$ be the evolution under TEP decoding of the average variable and check node degrees when the channel realization is \mathbf{y} . For any vector \mathbf{y} , $\Lambda_{\text{avg}}(t, \mathbf{y}, \mathcal{C})$ and $\Theta_{\text{avg}}(t, \mathbf{y}, \mathcal{C})$ are bounded during the whole decoding process.

Proof: See Appendix C. ■

The boundedness property of the variable degree evolution under TEP decoding, proved in Lemma 2, has a significant impact in the complexity of the TEP decoder for LDPC codes:

Lemma 3: The complexity of the TEP algorithm for decoding LDPC codes of positive rate and finite maximum variable and check node degrees is of order $\mathcal{O}(n)$. Compared to the BP complexity, it differs at most in a constant complexity per iteration.

Proof: A step of the PD algorithm, summarized in the linear transformation in (97), has a constant complexity. Its overall complexity is this value by the number of steps, n .

By crossing (97) and (99), we observe that the removal of a degree-two check node in a step of the TEP is performed by a

basic PD operation followed by the summation of two columns of the code parity check matrix \mathbf{H} . The cost of this operation is given by the number of ones in both columns. For LDPC codes, this value is given at any time t by $2\Lambda_{\text{avg}}(t)$, where $\Lambda_{\text{avg}}(t)$ is the average variable degree at time t . By Lemma 2, $\Lambda_{\text{avg}}(t)$ is bounded regardless the code length and the channel realization. This proves that any TEP decoder iteration just adds a constant complexity to the PD cost per iteration. ■

C. Connection to previous works

A similar procedure for removing degree-two check nodes was considered in the analysis of accumulate-repeat-accumulate (ARA) LDPC codes [44], [11]. ARA codes were proposed to achieve channel capacity under BP decoding at bounded complexity. Roughly speaking, ARA codes are formed by the concatenation of an accumulate binary encoder, an irregular LDPC code and another accumulate binary encoder. In [45], [46], Pfister and Sason showed that ARA codes can be described for BEC as an equivalent irregular LDPC ensemble and hence they were able to compute the ARA BP threshold using standard techniques [10]. To obtain such equivalent LDPC ensemble, parity checks of degree two, corresponding to the accumulate encoding, were processed similarly to how the TEP decoder processes degree-two check nodes. Once they obtained the equivalent irregular LDPC ensemble, they just consider BP decoding. Nevertheless, we want to emphasize that the novelty of our proposal is twofold: first, we consider, describe and measure the effect of the removal of degree-two check nodes to improve the BP solution for any block code. And second, we have shown that the idea of propagating pairwise relationships can be extended for any binary DMC using the EP framework.

IV. TEP DECODER EXPECTED GRAPH EVOLUTION

Both the PD and the TEP decoder sequentially reduce the LDPC Tanner graph by removing check nodes of degree one or two. As a consequence, the decoding process yields a sequence of residual graphs. In [43], [15], it is shown that if we apply the PD to elements of an LDPC ensemble, then the sequence of *residual graphs* follows a typical path or expected evolution [11]. The authors described this path as the solution of a set of differential equations and characterized the typical deviation from it. Their analysis is based on a result on the evolution of (martingale) Markov processes due to Wormald [47].

In this section, we first introduce the Wormald's theorem and then particularize it to compute the expected evolution of the residual graphs for the TEP, which is used in the following to evaluate the decoder performance.

A. Wormald's theorem

Consider a discrete-time Markov random process $Z^{(a)}(t)$ with finite d -dimension state space $\mathcal{A}(Z)^d$ that depends on some parameter $a > 1$. Let $Z_i^{(a)}(t)$ denote the i -th component of $Z^{(a)}(t)$ for $i \in \{1, \dots, d\}$. Let \mathcal{D} be a subset of \mathbb{R}^{d+1} containing those vectors $[0, z_1, \dots, z_d]$ such that:

$$p\left(\frac{Z_i^{(a)}(t=0)}{a} = z_i, 1 \leq i \leq d\right) > 0, \quad (37)$$

We define the stopping time $t_{\mathcal{D}}$ to be the minimum time so that $(t/a, Z_1^{(a)}(t)/a, \dots, Z_d^{(a)}(t)/a) \notin \mathcal{D}$. Furthermore, let $f_i(\cdot)$ for $1 \leq i \leq d$, be functions from $\mathbb{R}^{d+1} \rightarrow \mathbb{R}$ such that the following conditions are fulfilled:

- 1) (Boundedness). There exists a constant Ω such that for all $i \leq d$ and $a > 1$,

$$\left|Z_i^{(a)}(t+1) - Z_i^{(a)}(t)\right| \leq \Omega, \quad (38)$$

for all $0 \leq t \leq t_{\mathcal{D}}$.

- 2) (Trend functions). For all $1 \leq i \leq d$ and $a > 1$,

$$\begin{aligned} \mathbb{E} \left[Z_i^{(a)}(t+1) - Z_i^{(a)}(t) \middle| Z^{(a)}(t) \right] \\ = f_i \left(\frac{t}{a}, Z_1^{(a)}(t)/a, \dots, Z_d^{(a)}(t)/a \right), \end{aligned} \quad (39)$$

for all $0 \leq t \leq t_{\mathcal{D}}$.

- 3) (Lipschitz continuity). For each $i \leq d$, the function $f_i(\cdot)$ is Lipschitz continuous on the intersection of \mathcal{D} with the half space $\{[t, z_1, \dots, z_d] : t \geq 0\}$, i.e., if $\mathbf{b}, \mathbf{c} \in \mathbb{R}^{d+1}$ belong to such intersection, then there exists a constant ν such that

$$|f_i(\mathbf{b}) - f_i(\mathbf{c})| \leq \nu \sum_{j=1}^{d+1} |b_j - c_j|. \quad (40)$$

Under these conditions, the following holds:

- For $[0, b_1, \dots, b_d] \in \mathcal{D}$, the system of differential equations

$$\frac{\partial z_i}{\partial \tau} = f_i(\tau, z_1, \dots, z_d), \quad i = 1, \dots, d, \quad (41)$$

has a unique solution in \mathcal{D} for $z_i(\tau) : \mathbb{R} \rightarrow \mathbb{R}$ with $z_i(0) = b_i, 1 \leq i \leq d$.

- There exists a constant δ such that

$$p\left(\left|Z_i^{(a)}(t)/a - z_i(t/a)\right| > \delta a^{-\frac{1}{6}}\right) < d a^{\frac{2}{3}} \exp(-a^{\frac{1}{3}}/2), \quad (42)$$

for $i = 1, \dots, d$ and for $0 \leq t \leq t_{\mathcal{D}}$, where $z_i(\tau)$ is the solution given by equation (41) for

$$z_i(0) = \mathbb{E}[Z_i^{(a)}(t=0)/a]. \quad (43)$$

The result in (42) states that each realization of the process $Z_i^{(a)}(t)$ has a deviation from the solution of (41) smaller than $\mathcal{O}(a^{-1/6})$ if a is large enough. Our goal is to show that this theorem is suitable to describe the LDPC graph evolution during the TEP decoding process in certain scenarios.

B. LDPC ensembles and residual graphs

In this subsection, we introduce some basic notation about LDPC ensembles. An ensemble of codes, denoted by

LDPC $[\lambda(x), \rho(x), n]$, is defined by the code length n and the edge degree distribution (DD) pair $(\lambda(x), \rho(x))$ [10]:

$$\lambda(x) = \sum_{i=2}^{i_{\max}} \lambda_i x^{i-1}, \quad (44)$$

$$\rho(x) = \sum_{j=2}^{j_{\max}} \rho_j x^{j-1}, \quad (45)$$

where λ_i represents the fraction of edges with left degree i in the graph and ρ_j is the fraction of edges with right degree j . The left (right) degree of an edge is the degree of the variable (check) node it is connected to. The graph is specified in terms of fractions of edges, and not nodes, of each degree; this form is more convenient to analyze the convergence properties of the decoder. If the total number of edges in the graph is denoted by E , it can be readily checked that

$$E = \frac{n}{\sum_i \lambda_i / i}. \quad (46)$$

The design rate of the LDPC ensemble $r = r(\lambda(x), \rho(x))$ is set as follows [11]:

$$r = 1 - \frac{\Lambda_{\text{avg}}}{\Theta_{\text{avg}}}, \quad (47)$$

where Λ_{avg} and Θ_{avg} are, respectively, the average variable degree and the average check node degree in the graph. They can be computed from the graph DD:

$$\Lambda_{\text{avg}} = \frac{1}{\int_0^1 \lambda(\nu) d\nu}, \quad (48)$$

$$\Theta_{\text{avg}} = \frac{1}{\int_0^1 \rho(\nu) d\nu}. \quad (49)$$

To analyze the expected graph evolution, each time step corresponds to each step of the decoder. $L_i(t)$ and $R_j(t)$ are, respectively, the number of edges with left degree i and right degree j in the residual graph at time t and we define $l_i(t) = L_i(t)/E$ and $r_j(t) = R_j(t)/E$. We denote by $e(t)$ the number of edges in the graph at time t normalized by E . Hence, $l_i(t)/e(t)$ for $i = 1, \dots, i_{\max}(t)$ and $r_j(t)/e(t)$ for $j = 1, \dots, j_{\max}$ are the coefficients of the DD pair that defines the graph at time t . As we show in the next subsection, an small fraction of degree-one variable nodes might appear during the decoding process. Note that we have included an explicit dependency with time in $i_{\max}(t)$. As we described in Section III-A, the removal of degree-two check nodes tends to increase the variable degree and, consequently, we expect the maximum left degree to grow.

The remaining graph at time $t+1$ only depends on the graph at time t and, hence, the sequence of graphs $(L(t), R(t))$ along the time is a discrete time Markov process, where $L(t) = \{L_i(t)\}_{i=1}^{i_{\max}(t)}$, $R(t) = \{R_j(t)\}_{j=1}^{j_{\max}}$. It can be shown that the DD sequence of the residual graphs constitutes a sufficient statistic [15], [18] for this Markov process and, therefore, it suffices to analyze their evolution.

For a given LDPC ensemble and a BEC with parameter ϵ , the TEP decoder performance is analyzed and predicted using the expected evolution of $r_1(t)$ and $r_2(t)$ along the time. In

this section, we first identify their dependence with the rest of the components of the DD in the graph. Then, we show the conditions in which they can be estimated along the time using Worlmal's theorem.

C. Expected graph evolution in one TEP iteration

We analyze the average evolution of the DD pair $(L(t), R(t))$ in one iteration of the TEP decoder, i.e.

$$\mathbb{E}[L(t+1) - L(t) | L(t), R(t)], \quad (50)$$

$$\mathbb{E}[R(t+1) - R(t) | L(t), R(t)]. \quad (51)$$

At time t , the TEP looks for a check node of degree one or two to remove it. With probability

$$p_C(t) = \frac{R_1(t)}{R_1(t) + R_2(t)/2} \quad (52)$$

the decoder selects a check node of degree one, which is denoted as Scenario \mathcal{S}_1 . Alternatively, in Scenario \mathcal{S}_2 , a check node of degree two is removed with probability $\overline{p}_C(t) \doteq 1 - p_C(t)$. The expected variation of the process $(L(t), R(t))$ between t and $t+1$ can be expressed as follows:

$$\begin{aligned} \mathbb{E}[L_i(t+1) - L_i(t) | L(t), R(t)] = & \quad (53) \\ & \underbrace{p_C(t) \mathbb{E}[L_i(t+1) - L_i(t) | L(t), R(t), \mathcal{S}_1]}_I \\ & + \underbrace{\overline{p}_C(t) \mathbb{E}[L_i(t+1) - L_i(t) | L(t), R(t), \mathcal{S}_2]}_{II}, \end{aligned}$$

for $i = 1, \dots, i_{\max}(t)$ and

$$\begin{aligned} \mathbb{E}[R_j(t+1) - R_j(t) | L(t), R(t)] = & \quad (54) \\ & \underbrace{p_C(t) \mathbb{E}[R_j(t+1) - R_j(t) | L(t), R(t), \mathcal{S}_1]}_{III} \\ & + \underbrace{\overline{p}_C(t) \mathbb{E}[R_j(t+1) - R_j(t) | L(t), R(t), \mathcal{S}_2]}_{IV}, \end{aligned}$$

for $j = 1, \dots, j_{\max}$. In the following, we omit the pair $\{L(t), R(t)\}$ in the expectations to keep the notation uncluttered.

The terms I in (53) and III in (54) correspond to one iteration of the BP decoder and they were already computed in [15]. We include them for completeness:

$$\mathbb{E}[L_i(t+1) - L_i(t) | \mathcal{S}_1] = -i \frac{l_i(t)}{e(t)}, \quad (55)$$

for $i = 1, \dots, i_{\max}(t)$,

$$\begin{aligned} \mathbb{E}[R_j(t+1) - R_j(t) | \mathcal{S}_1] = & \quad (56) \\ j \left(\frac{r_{j+1}(t)}{e(t)} - \frac{r_j(t)}{e(t)} \right) (l_{\text{avg}}(t) - 1) - \delta(j-1) \end{aligned}$$

for $j = 1, \dots, j_{\max}$, where $\delta(j)$ is the Kronecker's delta function and

$$l_{\text{avg}}(t) = \sum_{i=1}^{i_{\max}(t)} i l_i(t) / e(t) \quad (57)$$

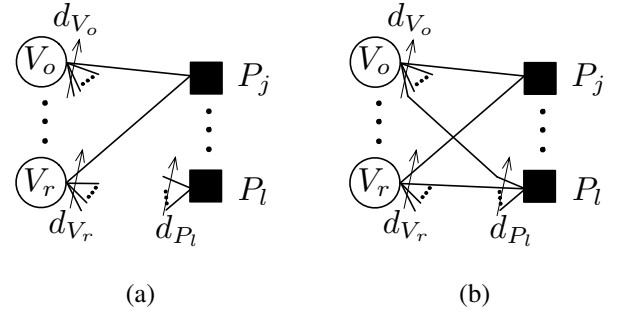


Fig. 4. Examples of Subscenarios \mathcal{S}_2^A in (a), given the check node P_j the variable nodes V_o and V_r only share the check node P_j , and \mathcal{S}_2^B in (b), in which they share another check node of degree d_{P_l} .

is the average edge left degree at time t . We now compute the terms II and IV in (53) and (54), respectively. When a check node of degree two is removed, e.g., P_j in Fig. 4, there are two possible subscenarios:

- \mathcal{S}_2^A : The variable nodes V_o and V_r connected with the check node P_j do not share another check node, depicted in Fig. 4(a).
- \mathcal{S}_2^B : The variable nodes V_o and V_r connected with the check node P_j share at least another check node, depicted in Fig. 4(b).

Let $p_B(t)$ be the probability of scenario \mathcal{S}_2^B , i.e., $p_B(t) = p(\mathcal{S}_2^B | \mathcal{S}_2)$. In Appendix B, we show that this probability is given by:

$$p_B(t) = \frac{(l_{\text{avg}}(t) - 1)^2 (r_{\text{avg}}(t) - 1)}{e(t)E}, \quad (58)$$

where

$$r_{\text{avg}}(t) = \sum_{j=1}^{j_{\max}} j r_j(t) / e(t) \quad (59)$$

is the average edge right degree. In Appendix B, we also show that the scenario \mathcal{S}_2^B is dominated by the case where the two variables connected to a check node of degree two only share another check node, as illustrated in Fig. 4(b). To compute II and IV in (53) and (54), we first evaluate the graph expected variation for \mathcal{S}_2^A and \mathcal{S}_2^B and then average them using $p_B(t)$:

$$\begin{aligned} \mathbb{E}[L_i(t+1) - L_i(t) | \mathcal{S}_2] = & p_B(t) \mathbb{E}[L_i(t+1) - L_i(t) | \mathcal{S}_2^B] \\ & + \overline{p}_B(t) \mathbb{E}[L_i(t+1) - L_i(t) | \mathcal{S}_2^A], \end{aligned} \quad (60)$$

$$\begin{aligned} \mathbb{E}[R_j(t+1) - R_j(t) | \mathcal{S}_2] = & p_B(t) \mathbb{E}[R_j(t+1) - R_j(t) | \mathcal{S}_2^B] \\ & + \overline{p}_B(t) \mathbb{E}[R_j(t+1) - R_j(t) | \mathcal{S}_2^A], \end{aligned} \quad (61)$$

where $\overline{p}_B(t) = 1 - p_B(t)$. Now we evaluate each term in (60) and (61).

1) *Expected graph variation assuming \mathcal{S}_2^A* : At time t , we remove the check node P_j in Fig. 4(a), which is connected to V_o and V_r . If V_o is the remaining variable, its degree becomes $d_{V_o} + d_{V_r} - 2$. Recall that d_{V_o} denotes the degree of variable node V_o . From the edge perspective, the graph losses d_{V_o} edges with left degree d_{V_o} and d_{V_r} edges with left degree d_{V_r} , and gains $d_{V_o} + d_{V_r} - 2$ edges with left degree $d_{V_o} + d_{V_r} - 2$. Note also that we have the same result if V_r is the remaining

variable. The node degrees d_{V_o} and d_{V_r} are asymptotically pairwise independent [48] and, thus, V_o and V_r are degree i with probability $l_i(t)/e(t)$ for $i = 1, \dots, i_{\max}(t)$.

We first focus on the evolution in the number of edges with left degree $i \geq 3$ at time $t + 1$, i.e. $L_i(t + 1)$. The sample space of $L_i(t + 1) - L_i(t)$ is given by:

$$L_i(t + 1) - L_i(t) \in \{-i, -2i, +i, 0\} \quad i \geq 3, \quad (62)$$

where

- $L_i(t + 1) - L_i(t) = -i$, if $(d_{V_o} = i \text{ XOR } d_{V_r} = i)$ AND $d_{V_o} + d_{V_r} - 2 \neq i$.
- $L_i(t + 1) - L_i(t) = -2i$, if $d_{V_o} = d_{V_r} = i$.
- $L_i(t + 1) - L_i(t) = +i$, if $d_{V_o} \neq i, d_{V_r} \neq i$ AND $d_{V_o} + d_{V_r} - 2 = i$.
- $L_i(t + 1) - L_i(t) = 0$, otherwise.

The probability associated to each case can be easily evaluated. Finally, the expected variation in the number of edges with left degree yields:

$$\begin{aligned} \mathbb{E}[L_i(t + 1) - L_i(t) | \mathcal{S}_2^A] = & \\ & -i \frac{l_i(t)}{e(t)} 2 \left(1 - \frac{l_i(t)}{e(t)} - \frac{l_2(t)}{e(t)} \right) - 2i \left(\frac{l_i(t)}{e(t)} \right)^2 \\ & + i \sum_{q=1}^{i+1} \frac{l_q(t)}{e(t)} \frac{l_{(i-q)+2}(t)}{e(t)}. \end{aligned} \quad (63)$$

For $i = 2$, the sample space reduces to $L_2(t + 1) - L_2(t) \in \{-2, +2, 0\}$ and, it is straightforward to show that:

$$\begin{aligned} \mathbb{E}[L_2(t + 1) - L_2(t) | \mathcal{S}_2^A] = & \\ & -2 \frac{l_2(t)}{e(t)} 2 \left(1 - \frac{l_2(t)}{e(t)} \right) - 2 \left(\frac{l_2(t)}{e(t)} \right)^2 + 2 \left(\frac{l_1(t)}{e(t)} \frac{l_3(t)}{e(t)} \right). \end{aligned} \quad (64)$$

For the case $i = 1$, we have

$$\begin{aligned} \mathbb{E}[L_1(t + 1) - L_1(t) | \mathcal{S}_2^A] = & \\ & -2 \frac{l_1(t)}{e(t)} \left(1 - \frac{l_2(t)}{e(t)} \right) - 2 \left(\frac{l_1(t)}{e(t)} \right)^2. \end{aligned} \quad (65)$$

Note that degree-one variable nodes are not created in both scenarios \mathcal{S}_1 and \mathcal{S}_2^A . Regarding the edge right degree distribution, only two edges of right degree two are lost and, hence,

$$\mathbb{E}[R_2(t + 1) - R_2(t) | \mathcal{S}_2^A] = -2, \quad (66)$$

$$\mathbb{E}[R_j(t + 1) - R_j(t) | \mathcal{S}_2^A] = 0, \quad j \neq 2. \quad (67)$$

2) *Expected graph variation assuming \mathcal{S}_2^B* : We study now the scenario depicted at Fig. 4(b), where the variables V_o and V_r are also linked to another check node P_l of degree d_{P_l} . In this case, the degree of the remaining variable is $d_{V_o} + d_{V_r} - 4$ and the check node P_l losses two edges and its degree reduces to $d_{P_l} - 2$. On the left side, the graph losses d_{V_o} edges with left degree d_{V_o} and d_{V_r} edges with left degree d_{V_r} , and gains $d_{V_o} + d_{V_r} - 4$ edges with left degree $d_{V_o} + d_{V_r} - 4$.

For a given degree $i \neq 4$, $L_i(t + 1) - L_i(t)$ takes value in the set in (62). The possible combinations of d_{V_o}, d_{V_r} and the associated $L_i(t + 1) - L_i(t)$ values are now as follows:

- $L_i(t + 1) - L_i(t) = -i$, if $(d_{V_o} = i \text{ XOR } d_{V_r} = i)$ AND $d_{V_o} + d_{V_r} - 4 \neq i$.
- $L_i(t + 1) - L_i(t) = -2i$, if $d_{V_o} = d_{V_r} = i$.
- $L_i(t + 1) - L_i(t) = +i$, if $d_{V_o} \neq i, d_{V_r} \neq i$ AND $d_{V_o} + d_{V_r} - 4 = i$.
- $L_i(t + 1) - L_i(t) = 0$, otherwise.

The expected value of $L_i(t + 1) - L_i(t)$ for $i \neq 4$ is given by:

$$\begin{aligned} \mathbb{E}[L_i(t + 1) - L_i(t) | \mathcal{S}_2^B] = & \\ & -i \frac{l_i(t)}{e(t)} 2 \left(1 - \frac{l_i(t)}{e(t)} - \frac{l_4(t)}{e(t)} \right) - 2i \left(\frac{l_i(t)}{e(t)} \right)^2 \\ & + i \sum_{q=1}^{i+3} \frac{l_q(t)}{e(t)} \frac{l_{(i-q)+4}(t)}{e(t)}, \end{aligned} \quad (68)$$

and, for the case $i = 4$ we obtain:

$$\begin{aligned} \mathbb{E}[L_4(t + 1) - L_4(t) | \mathcal{S}_2^B] = & \\ & -4 \frac{l_4(t)}{e(t)} 2 \left(1 - \frac{l_4(t)}{e(t)} \right) - 4 \left(\frac{l_4(t)}{e(t)} \right)^2 \\ & + 4 \sum_{q=1}^{i+3} \frac{l_q(t)}{e(t)} \frac{l_{(i-q)+4}(t)}{e(t)}. \end{aligned} \quad (69)$$

The values of i for which the number of edges involved in (63) and (68) is larger than the number of edges in the graph are not permitted. We set a zero probability for them. We do not enumerate the complete list of these combinations for the sake of the readability of the section.

The importance of scenario \mathcal{S}_2^B lies on the fact that the check node P_l losses two edges and its degree reduces to $d_{P_l} - 2$. Therefore, check nodes with right degree one can be created. Since the check node has degree $d_{P_l} = l$ with probability $r_l(t)/e(t)$, it can be shown that:

$$\mathbb{E}[R_j(t + 1) - R_j(t) | \mathcal{S}_2^B] = j \left(\frac{r_{j+2}(t)}{e(t)} - \frac{r_j(t)}{e(t)} \right), \quad (70)$$

for $j > 2$,

$$\mathbb{E}[R_2(t + 1) - R_2(t) | \mathcal{S}_2^B] = 2 \left(\frac{r_4(t)}{e(t)} - \frac{r_2(t)}{e(t)} \right) - 2, \quad (71)$$

and

$$\mathbb{E}[R_1(t + 1) - R_1(t) | \mathcal{S}_2^B] = \frac{r_3(t)}{e(t)}. \quad (72)$$

With the results in (63)-(72) and the probability $p_B(t)$ in (58), we are able to compute the terms II and IV in (53) and (54), obtaining the expected graph evolution in one iteration of the TEP decoder. It is important for the following analysis to note that, in any possible scenario, $R_1(t)$ and $R_2(t)$ only depend on the left DD through $l_{\text{avg}}(t)$.

D. Analysis of $l_{\text{avg}}(t)$ in the asymptotic limit

The application of Wormald's Theorem to guarantee the concentration around the TEP expected graph evolution derived in the previous subsection is not formally possible in the limit $n \rightarrow \infty$. First, the maximum left degree $i_{\text{max}}(t)$ is not bounded and the boundedness condition in (38) might not hold. And second, note that the dimension of the Markov process $\{L(t), R(t)\}$ is not bounded either. However, the asymptotic limit performance can be studied by observing the evolution of the average left degree $l_{\text{avg}}(t)$, which measures how likely is the creation of degree-one check nodes by removing degree-two check nodes, see Fig. 3.

If we assume an LDPC $[\lambda(x), \rho(x), n]$ ensemble with bounded complexity, i.e. finite $\lambda_{\text{avg}}, i_{\text{max}}$ and j_{max} values, then in the limit $n \rightarrow \infty$ we get $p_B(t=0) = 0$. As long as $p_B(t) = 0$, the TEP and BP solutions are equivalent. Therefore, the BP decoding threshold is only improved for those LDPC ensembles for which, as the TEP decoder runs, there exists some $t_0 \leq t_D$ such that

$$\lim_{t \rightarrow t_0} \lim_{n \rightarrow \infty} p_B(t) = \lim_{t \rightarrow t_0} \lim_{n \rightarrow \infty} \frac{(l_{\text{avg}}(t) - 1)^2 (r_{\text{avg}}(t) - 1) \sum_i \lambda_i / i}{e(t)n} > 0 \quad (73)$$

or, equivalently, if there exists some $t_0 \leq t_D$ such that

$$\lim_{t \rightarrow t_0} l_{\text{avg}}(t) = \infty, \quad (74)$$

since the rest of the terms in (73) stay bounded during the TEP procedure if $\epsilon \geq \epsilon_{\text{BP}}$. If $l_{\text{avg}}(t)$ becomes infinite, the asymptotic decoding threshold for the TEP might be higher than the decoding threshold of the BP decoder. However, we cannot rely on Wormald's Theorem to find the TEP threshold ϵ_{TEP} .

In this section, we show the conditions that be need to be fulfilled by an LDPC ensemble to outperform the BP asymptotic limit, i.e. to get an infinite left-average degree $l_{\text{avg}}(t)$ under TEP decoding. During our research, we have not found any LDPC ensemble with finite degree distribution

meeting these conditions and, besides, the strategies followed to maximize this effect yield ensembles that lack of practical interest. We clarify this point at the end of the section and leave as an interesting open problem the search of codes practical LDPC ensembles for which $\epsilon_{\text{TEP}} > \epsilon_{\text{BP}}$ and the exact computation of such threshold.

Assume an LDPC ensemble of infinite length. As proven in Appendix A, the processing order is irrelevant and we can always run the BP first. The removal of degree-one check nodes does not increase the left average degree, i.e. $l_{\text{avg}}(t)$ is finite [11]. Over the BP residual graph, processing a degree-two check node can be explained with a Polya urn model. Consider $i_{\text{max}}(t)$ urns labeled $1, 2, \dots, i_{\text{max}}(t)$. In urn i we place a ball for each variable of degree i in the graph. In each iteration, we take two balls from the urns. The urns are chosen independently with probability proportional to the number of balls per urn times its label. One ball is thrown away and the other one is placed in the urn labeled by the sum of the labels of the picked balls minus 2, introducing a new urn if it did not previously exist. For example, if we pick a ball with label "3" and a ball with label "4", we put one ball in the urn labeled "5". We repeat this process c_2 times, the number of degree-two check nodes in the BP residual graph. The resulting $l_{\text{avg}}(t)$ is the sum of the number of balls in all urns multiplied by their labels.

It is straightforward to conclude that, as we process check nodes of degree two, $l_{\text{avg}}(t)$ increases, but does it becomes infinite? On the one hand, if we start with n' balls and $c_2 = n' - 1$, $l_{\text{avg}}(t)$ becomes infinite as $n' \rightarrow \infty$. On the other hand, if c_2 is small enough such that we do not pick twice the same ball, $l_{\text{avg}}(t)$ stays finite. There must be an intermediate value for c_2 for which $l_{\text{avg}}(t)$ becomes infinite.

Let us illustrate this result with the (3,6) regular LDPC code. We run the urn model described above to compute $l_{\text{avg}}(t)$. In Fig. 5(a), we plot $l_{\text{avg}}(t)$ for $n' = 10^2$ (\triangle), 10^3 (\times), 10^4 (\circ), 10^5 (\square), as a function of the fraction of processed variables c_2/n' . In Fig. 5(b) we plot the ratio between $l_{\text{avg}}(t)$ for $n' = 10^{j+1}$ and $n' = 10^j$ for $j = 2$ (\times), 3 (\circ) and 4 (\square).

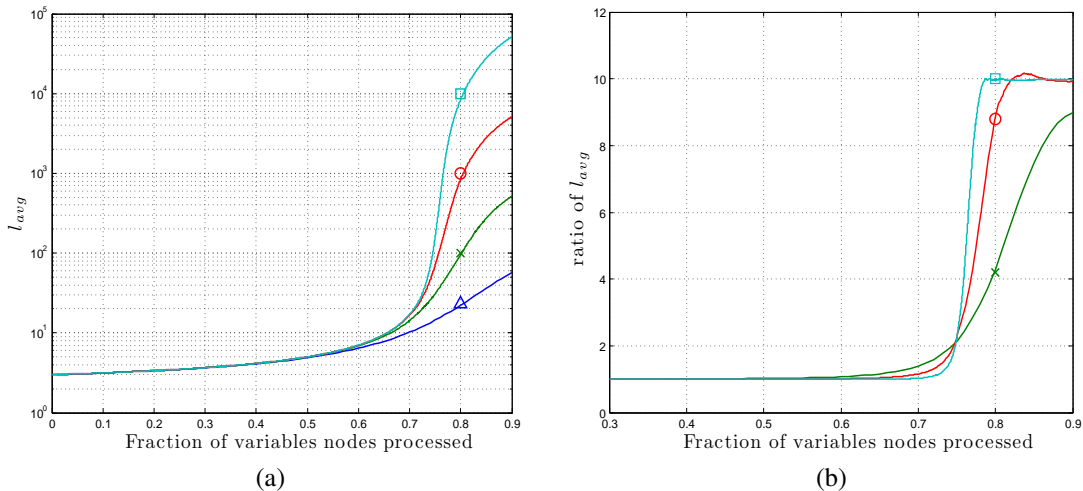


Fig. 5. In Fig. 5(a), we plot the average left degree $l_{\text{avg}}(t)$ computed using the urn model for $n' = 100$ (\triangle), 1000 (\times), 10^4 (\circ), 10^5 (\square), as a function of the fraction of processed variables. In Fig. 5(b) we plot the ratio between $l_{\text{avg}}(t)$ for $n' = 10^{j+1}$ and $n' = 10^j$ for $j = 2$ (\times), 3 (\circ) and 4 (\square).

Although the urn model is only valid asymptotically and as long as $p_B(t) = 0$, we can see there is a clear phase-transition. If we process less than 74% of the variables nodes we should not expect $l_{\text{avg}}(t)$ to go to infinity. For a BEC channel with erasure probability just above the BP threshold ($\epsilon = 0.4295$), the ratio between degree-two check nodes and variables in the BP residual graph is 0.625 [15]. Therefore, for this ensemble the TEP decoder performs asymptotically as the BP decoder, i.e. $\epsilon_{\text{TEP}} = \epsilon_{\text{BP}}$, because $l_{\text{avg}}(t)$ stays finite.

In order to maximize the fraction c_2 with respect to the number of variables in the BP residual graph there are two basic strategies. We can either design LDPC ensembles to minimize the size of the residual BP graph or we can design the ensemble to increase the presence of degree-two check nodes. Given the known analytical expressions for the BP residual graph [15], it is easy to prove that in the first case the solution yields standard irregular ensembles for which $\epsilon_{\text{BP}} \rightarrow \epsilon_{\text{MAP}}$, i.e. codes for which the threshold is given by the stability condition [14], [15], [21]. In this case, there is no margin and $\epsilon_{\text{BP}} = \epsilon_{\text{TEP}} = \epsilon_{\text{MAP}}$. In the second case, the ensemble presents severe limitations: for instance, by (47), any ensemble where all the check nodes are of degree two, i.e. $\rho(x) = x$, has a rate

$$r(\lambda(x), x) = 1 - \frac{2}{\int_0^1 \lambda(\nu) d\nu} \in [0, 1] \Rightarrow \lambda(x) = a + bx, \quad (75)$$

where $a, b \in \mathbb{R}$ are such that $a + b = 1$. Either the code presents minimum distance of only one bit if $a > 0$ or zero rate if $a = 0$. We approach this undesired behavior as we increase the fraction of degree-two check nodes ρ_2 .

E. TEP decoder differential equations

Unlike the asymptotic case, for finite-length LDPC ensembles such that $\epsilon_{\text{TEP}} = \epsilon_{\text{BP}}$, Wormald's Theorem can be applied to estimate the expected graph evolution along the decoding process. In particular, we are interested in the evolution of $r_1(t)$ and $r_2(t)$, which is basic to predict the finite-length performance as we later discuss in Section V.

Consider the TEP decoding of an arbitrarily large LDPC $[\lambda(x), \rho(x), n]$ ensemble with finite code length. First, note that expressions (53) and (54) play the role of the trend functions in Wormald's theorem:

$$\mathbb{E}[R_j(t+1) - R_j(t)] \quad (76)$$

$$= f_{R_j} \left(\frac{t}{E}, \frac{L_{\text{avg}}(t)}{E}, \frac{R_1(t)}{E}, \dots, \frac{R_{j_{\text{max}}}(t)}{E} \right),$$

$$\mathbb{E}[L_i(t+1) - L_i(t)] \quad (77)$$

$$= f_{L_i} \left(\frac{t}{E}, \frac{L(t)}{E}, \frac{R_1(t)}{E}, \frac{R_2(t)}{E} \right),$$

for $i = 1, \dots, E$ and $j = 1, \dots, j_{\text{max}}$, where $L_{\text{avg}}(t) = \sum_i i L_i(t)$. Regarding the bounding condition in (38), for finite ensembles, any individual realization $|R_j(t+1) - R_j(t)|$ and $|L_i(t+1) - L_i(t)|$ are bounded by E at any time. This condition also ensures the Lipschitz continuity of the functions $f_{L_i}(\mathbf{b})$ and $f_{R_j}(\mathbf{b})$ in (76) and (77) for all \mathbf{b} contained in the set

\mathcal{D} defined in (37). In this case, \mathcal{D} is simply the region of possible initial conditions for the DD, i.e. the region within the hypercube of unit length and dimension $E + j_{\text{max}}$.

Given the former discussion, Wormald's Theorem ensures that when we solve the differential equations:

$$\frac{\partial r_j(\tau)}{\partial \tau} = f_{R_j}(\tau, l_{\text{avg}}(\tau), r_1(\tau), \dots, r_{j_{\text{max}}}(\tau)), \quad (78)$$

$$\frac{\partial l_{\text{avg}}(\tau)}{\partial \tau} = \sum_i i f_{L_i}(\tau, l_2(\tau), \dots, l_E(\tau), r_1(\tau), r_2(\tau)), \quad (79)$$

$$\frac{\partial l_i(\tau)}{\partial \tau} = f_{L_i}(\tau, l_2(t), \dots, l_E(t), r_1(t), \dots, r_{j_{\text{max}}}(t)), \quad (80)$$

for $j = 1, \dots, j_{\text{max}}$ and $i = 1, \dots, E$ with initial conditions $l_i(0) = \mathbb{E}[L_i(0)]/E$ and $r_j(0) = \mathbb{E}[R_j(0)]/E$, then the solution for $r_1(\tau)$ and $r_2(\tau)$ is unique and, with high probability, by (42), does not differ more than $\mathcal{O}(E^{-1/6})$ from any particular realization of $R_j(t)/E$ for $j = 1, 2$. Because of the expected graph evolution equations derived in Section IV-C assumed independency, the deviation that we can expect with respect to the solution given by (78)-(80) might rise up to $\mathcal{O}(E^{-1/6} + E^{-1})$. As we show in Appendix B, any cycle involving m variables decays as E^{-m} . The most dominant component, i.e. E^{-1} , is not significant compared to maximum deviation guaranteed by Wormald's theorem.

Note that the initial conditions, $l_i(0)$ and $r_j(0)$, contain the information about the ensemble LDPC $[\lambda(x), \rho(x), n]$ and the channel [15], [11]:

$$l_i(0) = \epsilon \lambda_i, \quad i \leq i_{\text{max}}, \quad (81)$$

$$r_j(0) = \sum_{m \geq j} \rho_j \binom{m-1}{j-1} \epsilon^j (1-\epsilon)^{m-j}, \quad j = 1, \dots, j_{\text{max}}. \quad (82)$$

It is important to remark that, as described in Section IV-A, the solution of (78)-(79) only holds for all $t < t_{\mathcal{D}}$. In our scenario, the stopping time $t_{\mathcal{D}}$ is given by either the time instant at which the decoder stops because there are no degree-one or degree-two check nodes or the time when $e(\tau)$ cancels, denoting that all variables in the graph have been decoded.

Let us illustrate the accuracy of this model to analyze the TEP decoder properties for a very large code length, $n = 2^{17}$. In Fig. 6(a), we compare the solution of the system of differential equations in (78) and (79) for $R_1(\tau) = r_1(\tau)E$ and $R_2(\tau) = r_2(\tau)E$ for a regular (3,6) code with 20 particular decoding trajectories obtained through simulation. We consider two cases: below ($\epsilon = 0.415$) and above ($\epsilon = 0.43$) the BP threshold, i.e. $\epsilon_{\text{BP}} = 0.4294$. We depict their evolution along the residual graph at each time, i.e. $e(\tau)$. We plot in thick lines the solution of our model for $R_1(\tau)$ (\triangleleft) and $R_2(\tau)$ (\diamond), and in thin lines the simulated trajectories, $R_1(\tau)$ in solid and $R_2(\tau)$ in dashed line. In Fig. 6(b), we reproduce the same experiment for the following irregular LDPC ensemble,

$$\lambda(x) = \frac{1}{6}x + \frac{5}{6}x^3, \quad (83)$$

$$\rho(x) = x^5, \quad (84)$$

where the BP threshold for this code is $\epsilon_{\text{BP}} = 0.4828$. For this code, by running the urn model procedure described previously in Section IV-D, we also find that $l_{\text{avg}}(t)$ does not scale with n .

In both cases, when we are below the BP threshold both the expected evolution curves and the empirical trajectories represent successful decoding since degree-one check nodes do not vanish until $e(\tau)$ tends to zero. Besides, note also that the longest deviation happens around $\tau \approx 0.12$ and $\tau \approx 0.18$, when the predicted curves for both $R_1(\tau)$ and $R_2(\tau)$ have a relative minimum. This point is known as critical point and plays a fundamental role in the derivation of scaling laws to predict the performance in the finite length regime [18], [11], as explained in Section V.

In [18], [19], the authors show that the graph initial DD are Gaussian distributed around the mean in (81) and (82). Furthermore, they observe that as the PD performs, individual realizations are also Gaussian distributed around the mean computed in [15] using Wormald's theorem. And they show that the standard deviation is $\mathcal{O}(1/\sqrt{E})$, lower than the one

warranted by Wormald's theorem. This result is a consequence of the channel properties. In Fig. 6 we observe the same results for the TEP decoder.

V. TEP DECODING OF LDPC ENSEMBLES IN THE FINITE-LENGTH REGIME

A. Motivation

In [28], [29], we empirically observed the gain in performance obtained when the TEP decoder is applied to decode some finite-length LDPC ensembles over the BEC. The gain of the proposed algorithm for practical codes can be analyzed from a different perspective based on the recent work by Polyanskiy *et al.* [49]. They present bounds on the maximum achievable coding rate for binary memoryless channels in the finite-length regime. These bounds can be regarded as the extension of the Shannon coding rate limit when the number of channel uses, i.e. code length, is fixed. For a given channel, a target probability of error P_W and a desired code rate r , we can compute the minimum code length n_{min} for which there exists a code that satisfies these requirements.

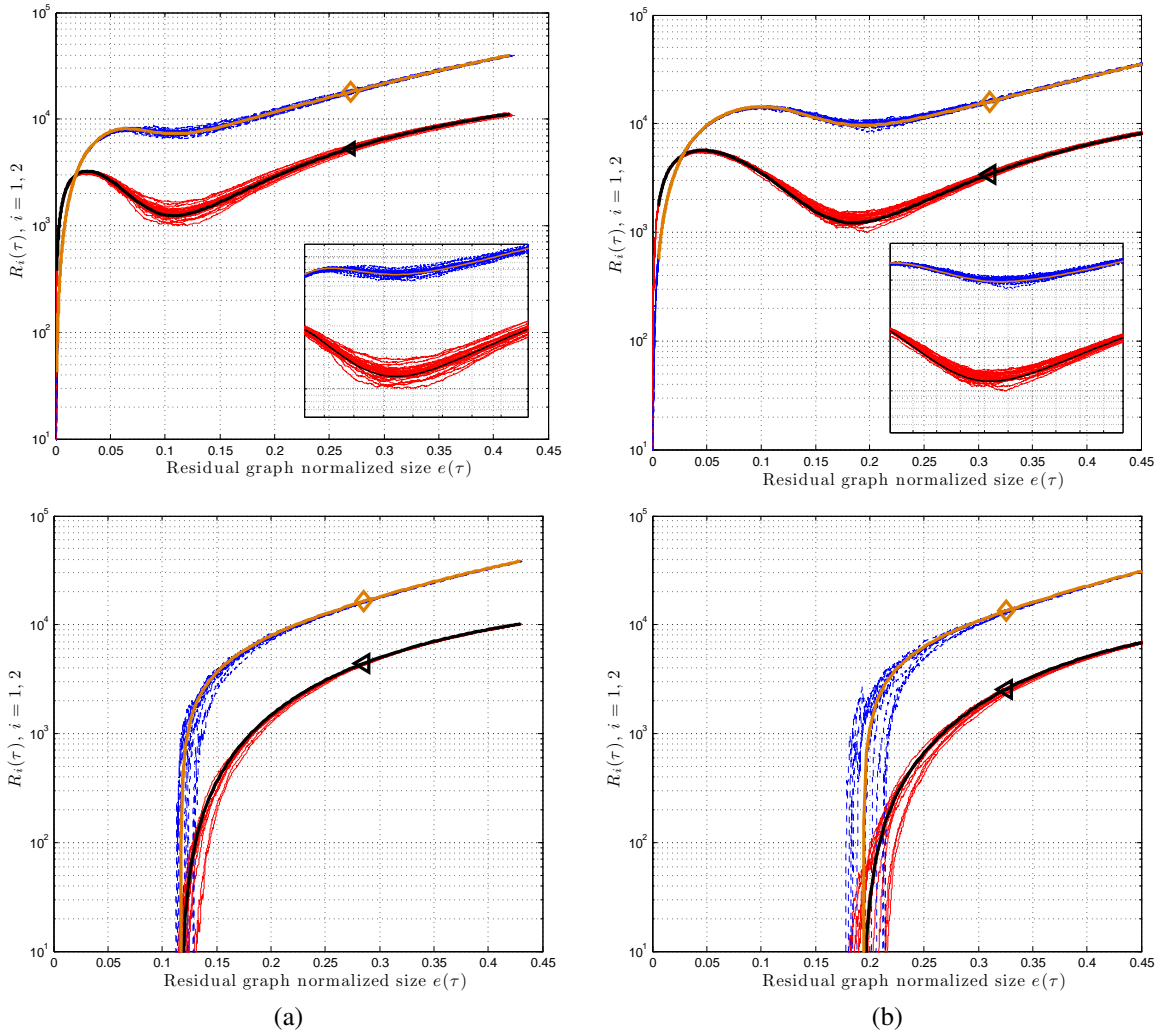


Fig. 6. In (a), we include the predicted evolution of $R_1(\tau)$ (\triangleleft) and $R_2(\tau)$ (\triangleleft) for a regular (3,6) code with $n = 2^{17}$ and an erasure probability $\epsilon = 0.415 < \epsilon_{\text{BP}}$ (top) and $\epsilon = 0.43 > \epsilon_{\text{BP}}$ (bottom), where $\epsilon_{\text{BP}} = 0.4294$. In (b), we include the same result for the irregular DD defined in (83) and (84) and an erasure probability $\epsilon = 0.47 < \epsilon_{\text{BP}}$ (top) and $\epsilon = 0.483 > \epsilon_{\text{BP}}$ (bottom), where $\epsilon_{\text{BP}} = 0.4828$. We include in thin lines a set of 20 individual decoding trajectories chosen at random.

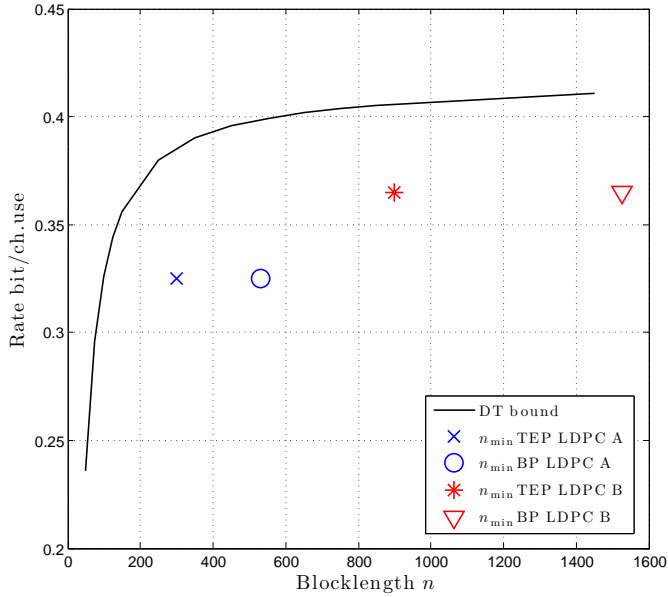


Fig. 7. Dependency-testing (DT) lower bound to the maximal rate achievable with maximal block error rate $P_W \leq 10^{-3}$ over a BEC of parameter $\epsilon = 0.5$ [49]. We include the minimum code length computed to obtain a valid performance for both the TEP and the BP and two LDPC ensembles A and B of rates $r_A = 0.325$ and $r_B = 0.365$.

In Fig. 7, we plot the dependency-testing (DT) lower bound to the maximal achievable rate for a target block error rate of $P_W = 10^{-3}$ over a BEC of parameter $\epsilon = 0.5$. In [49], this lower bound is shown to be tight and much simpler to compute than the non-asymptotic maximum achievable rate. We considered two LDPC ensembles, referred to as code A and B. In both codes, $\lambda(x) = x^2$, while $\rho_A(x) = 0.25x^3 + 0.75x^4$ and $\rho_B(x) = 0.5x^3 + 0.5x^4$. The rate of each code is, respectively, $r_A = 0.325$ and $r_B = 0.365$. In Fig. 7, we depict the minimum code length for both the TEP and the BP decoders to empirically obtain a performance below 10^{-3} for each one of the two LDPC ensembles proposed. We can observe the use of the TEP decoder reduces by roughly half the block length to the optimum case given by the DT bound. Since the complexity of both algorithms is of the same order, the TEP decoder emerges as a powerful method to decode practical finite-length LDPC codes.

B. Gain in the finite-length regime

We now focus on the TEP decoder improvement in performance for finite-length codes with respect to the BP solution, which can be predicted using the solution of the TEP differential equations in Section IV. We also extend the SL for the BP proposed in [18], [19], [20] to the TEP decoder. We are able to predict the performance for a given LDPC ensemble in the waterfall region.

In [18], [19], the authors proved that the BP performance for finite-length LDPC codes can be predicted by analyzing the statistical presence of degree-one check nodes at a finite set of time instants during the whole decoding process. These points are referred to as *critical points*:

Definition 1: BP-critical point of an LDPC ensemble. For

a given LDPC ensemble with $n \rightarrow \infty$ and BP threshold ϵ_{BP} , let $r_1^{BP}(\tau)$ be the expected evolution of the fraction of degree-one check nodes under BP decoding at ϵ . We say that τ^* is a BP-critical point of the LDPC ensemble if

$$\lim_{\epsilon \rightarrow \epsilon_{BP}^-} r_1^{BP}(\tau^*) = 0. \quad (85)$$

In [15], [43], the authors analytically compute $r_1^{BP}(\tau)$ as a function of the LDPC degree distribution and the channel parameter ϵ :

$$r_1^{BP}(u) = \epsilon \lambda(u) \left(u - 1 + \rho(1 - \epsilon \lambda(u)) \right), \quad (86)$$

where

$$\frac{\partial u}{u} = \frac{-\partial \tau}{e(\tau)} \Rightarrow u = \exp \left(- \int_0^\tau \frac{ds}{e(s)} \right). \quad (87)$$

Given the parameter u in (87), the decoding process starts at $u = 1$ and finishes at $u = 0$.

In [18], [19], the authors show that BP decoding trajectories for finite-length values present the average in (86) and a variance that decreases by $\mathcal{O}(n^{-1})$. In addition, it is shown the BP decoder at $\epsilon = \epsilon_{BP} + \Delta\epsilon$ succeed with very high probability as long as there exists a positive fraction of degree-one check nodes at the critical points, computed from (86). The finite-length performance is estimated by computing the cumulative probability distribution of individual trajectories at the critical points. We show that the same idea extends to the TEP case.

For the TEP decoder, the analysis of the finite-length performance for a given ensemble can be restricted as well to a discrete set of time instants. By extension we call them *TEP-critical points*:

Definition 2: TEP-critical point of an LDPC ensemble. For a given LDPC ensemble with $n \rightarrow \infty$ and TEP threshold $\epsilon_{TEP} = \epsilon_{BP}$, let $r_1(\tau)$ be the expected evolution of the fraction of degree-one check nodes under TEP decoding. We say that τ' is a TEP-critical point of the LDPC ensemble if

$$\lim_{\epsilon \rightarrow \epsilon_{TEP}^-} r_1(\tau') = 0. \quad (88)$$

Lemma 4: For a given ensemble LDPC $[\lambda(x), \rho(x), n \rightarrow \infty]$, the number of TEP critical points is equal to the number of BP critical points.

Proof: For the regime $n \rightarrow \infty$, we have proved that the TEP decoder is not able to create any additional check nodes of degree one with respect to the BP solution and, as a consequence, $\epsilon_{TEP} = \epsilon_{BP}$. Besides, given the TEP independence of the processing order proved in Appendix A, we can implement the TEP decoder by first removing all the degree-one check nodes, i.e. a BP stage, and then process degree-two check nodes if the BP does not succeed. For $\epsilon \rightarrow \epsilon_{BP}^-$ and $n \rightarrow \infty$, $r_1^{BP}(\tau)$ and $r_1(\tau)$ match during the whole decoding process and, therefore, the ensemble presents the same number of critical points for both decoding algorithms. ■

To estimate the TEP performance, we compute the cumulative probability distribution of decoding trajectories at the critical points. The TEP decoder gain in performance for

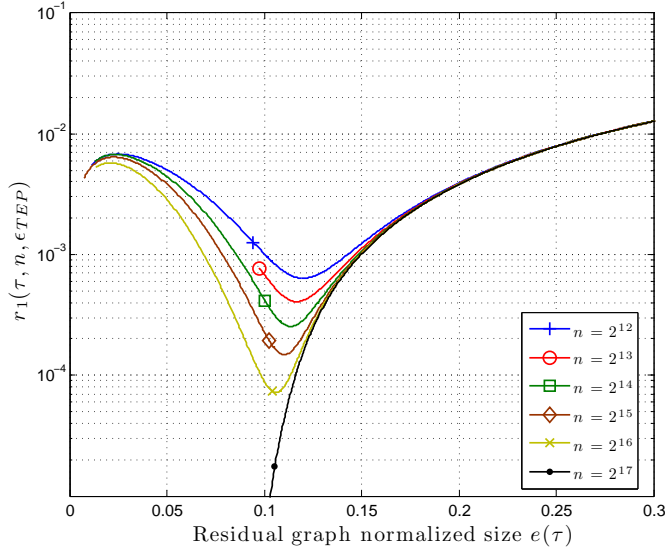


Fig. 8. We plot the solution for $r_1(\tau)$ along with $e(t)$ given by the solution of (78)-(79) for a $(3, 6)$ regular code at $\epsilon = \epsilon_{BP} = \epsilon_{TEP}$. The code lengths considered are $n = 2^{12}$ (+), $n = 2^{13}$ (o), $n = 2^{14}$ (□), $n = 2^{15}$ (◇), $n = 2^{16}$ (x) and $n = 2^{17}$ (•).

finite-length codes can be explained as: for a given finite-length ensemble LDPC $[\lambda(x), \rho(x), n]$, the expected graph evolution computed in (78)-(79) provides the average presence of degree-one check nodes at any time τ , i.e. $r_1(\tau, n, \epsilon)^5$. Unlike the BP case in (86), the average trajectory $r_1(\tau, n, \epsilon)$ is strongly dependent on the code length n . Individual trajectories for shorter codes present higher mean values at the critical points so that the cumulative distribution is significantly higher than for the BP counterpart.

For instance, in Fig. 8, we include the solution for $r_1(\tau, n, \epsilon)$ for the $(3, 6)$ regular code at $\epsilon = \epsilon_{BP} = \epsilon_{TEP}$. The code lengths considered are $n = 2^{12}$ (+), $n = 2^{13}$ (o), $n = 2^{14}$ (□), $n = 2^{15}$ (◇), $n = 2^{16}$ (x) and $n = 2^{17}$ (•). For $n \geq 2^{17}$, we can approximately locate the single TEP-critical point of the ensemble: $r_1(\tau', n, \epsilon_{BP})$ cancels at $e(\tau) \approx 0.1$. For lower code lengths, $r_1(\tau', n, \epsilon_{TEP})$ does not vanish since the graph is small enough to make $p_B(t)$ in (58) significant. The fraction $r_1(\tau', n, \epsilon_{TEP})$ represents the number of degree-one check nodes that the TEP decoder is able to create with respect to the BP solution, which is zero at the critical point. As we increase the codeword length, we eventually observe that $r_1(\tau', n, \epsilon_{TEP})$ cancels, which indicates that, above this code length, we do not expect any significant improvement between the BP and the TEP solution.

In addition, a closer look to the curves in Fig. 8 shows that $r_1(\tau', n, \epsilon_{TEP})$ decays approximately as $\mathcal{O}(1/n)$, which is in consistency with probability $p_B(t)$ in (58):

$$r_1(\tau', n, \epsilon_{TEP}) \approx \gamma_{TEP} n^{-1}, \quad (89)$$

where γ_{TEP} depends on the ensemble. We obtain this value by linearly interpolating $r_1(\tau', n, \epsilon_{TEP})^{-1}$ for different code lengths. We propose the following method to accurately com-

⁵To avoid any confusion, in the following, we explicitly include the dependence with n and ϵ .

pute $r_1(\tau', n, \epsilon_{TEP})$ for each code length. It is based on the TEP solution independency of the processing order, see Appendix A:

- Start the TEP algorithm by running a BP stage. Compute the BP residual graph expected DD at $\epsilon = \epsilon_{BP}$ [15]. Alternatively, we can obtain such DD by evaluating the differential equations for the TEP in (78)-(79) if we set $p_C(\tau) = 1$ in (52) for any τ until the fraction of degree-one check nodes in the graph cancels.
- Using this graph as input, evaluate the graph expected evolution when we only remove degree-two check nodes: solve the system (78)-(79) by setting $p_C(\tau) = 0$ in (52) for all τ until the graph runs out of degree-two check nodes.
- $r_1(\tau', n, \epsilon_{TEP})$ is the remaining fraction of degree-one check nodes in the final graph.

In Fig. 9, we represent the evolution of $r_1(\tau, n, \epsilon_{TEP})$ after following the previous steps for the regular $(3, 6)$ -LDPC code and $n = 2^{12}$ (+), $n = 2^{14}$ (□) and $n = 2^{16}$ (x). By (86), the three curves overlap under BP during the BP stage. At $e(\tau) \approx 0.22$, the BP decoder gets stuck and we begin to remove degree-two check nodes. By interpolating the $r_1(\tau', n, \epsilon_{TEP})$ estimation for a set of code lengths we obtain $\gamma_{TEP}^{-1} = 0.3194$. If we consider other LDPC ensembles of single critical points, we observe that (89) is a general property, where the constant γ_{TEP} depends on the ensemble. For instance, for the irregular LDPC ensemble in (83) and (84), we computed $\gamma_{TEP}^{-1} = 0.2925$.

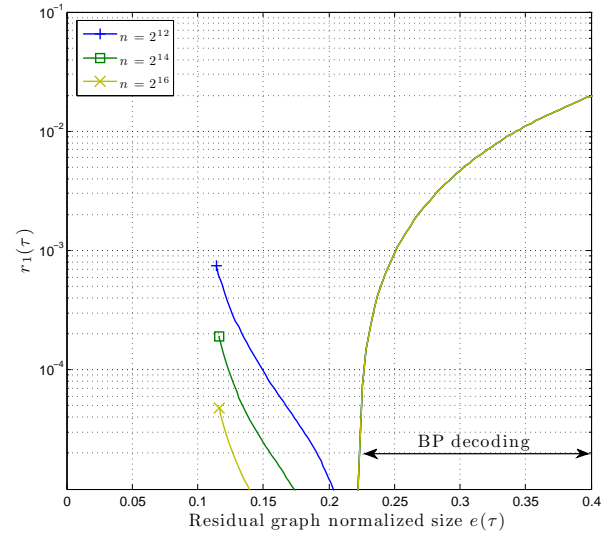


Fig. 9. We plot the solution for $r_1(\tau)$ computed to estimate $r_1(\tau', n, \epsilon_{TEP})$ for a $(3, 6)$ regular code at $\epsilon = \epsilon_{BP} = \epsilon_{TEP}$. The code lengths considered are $n = 2^{12}$ (+), $n = 2^{14}$ (□) and $n = 2^{16}$ (x). The BP was first run and the degree-two check nodes are processed.

C. BP SL for single critical-point LDPC ensembles

In [18], it was proposed the following SL to predict the BP error performance of LDPC ensembles with one single critical point. Consider a transmission over the BEC using random elements from an ensemble LDPC $[\lambda(x), \rho(x), n]$ which has

a single non-zero critical point. Let $\epsilon_{BP} = \epsilon_{BP}(\lambda(x), \rho(x))$ denote the BP threshold. Then,

$$\mathbb{E}_{\text{LDPC}[\lambda(x), \rho(x), n]} [P_W^{\text{BP}}(\mathcal{C}, \epsilon)] = \mathcal{Q}\left(\frac{\sqrt{n}(\epsilon_{BP} - \beta_{BP}n^{-2/3} - \epsilon)}{\alpha_{BP}}\right) \left(1 + \mathcal{O}(n^{-1/3})\right), \quad (90)$$

where $P_W^{\text{BP}}(\mathcal{C}, \epsilon)$ is the average block error probability for the code $\mathcal{C} \in \text{LDPC}[\lambda(x), \rho(x), n]$, $\alpha_{BP} = \alpha_{BP}(\lambda(x), \rho(x))$ and $\beta_{BP} = \beta_{BP}(\lambda(x), \rho(x))$. The analytical expression for the parameters α_{BP} and β_{BP} can be found in [18], [20].

It is important for our work to provide further details about the derivation of the SL in (90). For $\epsilon = \epsilon_{BP}$, we know by assumption that there exists just only one critical point τ^* such that $r_1^{\text{BP}}(\tau^*) = 0$. If we now vary ϵ slightly, the expected fraction of check nodes at τ^* can be estimated by Taylor expansion around this point:

$$r_1^{\text{BP}}(\tau^*) = \left. \frac{\partial r_1^{\text{BP}}(\tau)}{\partial \epsilon} \right|_{\substack{\tau=\tau^* \\ \epsilon=\epsilon_{BP}}} \Delta \epsilon, \quad (91)$$

where $\Delta \epsilon = (\epsilon - \epsilon_{BP})$. As we discussed in Section IV-E, because of the channel dispersion, individual decoding trajectories are asymptotically Gaussian distributed around the solution given by the graph expected evolution with a variance of order $\mathcal{O}(1/n)$ [11], [18]. Hence, at point τ^* , the observed fraction of degree-one check nodes is a normal random variable with mean given in (91) and variance denoted by $\delta_{r_1, r_1}^{\text{BP}}(\tau^*)/n$. A coarse estimation of the error probability is obtained by computing the probability that this random variable is less than zero:

$$\mathbb{E}_{\text{LDPC}[\lambda(x), \rho(x), n]} [P_W^{\text{BP}}(\mathcal{C}, \epsilon)] \approx 1 - \mathcal{Q}\left(\frac{\left. \frac{\partial r_1^{\text{BP}}(\tau)}{\partial \epsilon} \right|_{\substack{\tau=\tau^* \\ \epsilon=\epsilon_{BP}}} \Delta \epsilon}{\sqrt{\delta_{r_1, r_1}^{\text{BP}}(\tau^*)/n}}\right) = \mathcal{Q}\left(\frac{\sqrt{n}(\epsilon_{BP} - \epsilon)}{\alpha_{BP}}\right), \quad (92)$$

where

$$\alpha_{BP} = \sqrt{\delta_{r_1, r_1}^{\text{BP}}(\tau)} \left(\left. \frac{\partial r_1^{\text{BP}}(\tau)}{\partial \epsilon} \right) \right|_{\substack{\tau=\tau^* \\ \epsilon=\epsilon_{BP}}}^{-1}. \quad (93)$$

For sufficiently large code lengths, the scaling function in (92) provides an accurate estimation of the BP error probability [18], [19]. However, for moderately size block-lengths, we are underestimating the error probability since we ignore those trajectories for which the fraction of check nodes of degree one cancels at $\tau \leq \tau^*$. A deeper analysis shows that this effect can be included in the scaling function by introducing the β_{BP} parameter in (90).

D. TEP SL for single critical-point LDPC ensembles

We now show that the TEP decoder can be modeled by a similar scaling law and we provide a first estimate of the scaling parameters as a function of the LDPC DD.

As discussed at the beginning of this section, $r_1(\tau, n, \epsilon_{BP})$ provides the average presence of degree-one check nodes at the codes's critical point for finite-length sizes. Then, we proceed

as in (91)-(93) to estimate the TEP error probability. Consider the standard implementation of the decoder, for which degree-one and two check nodes are alternatively removed. The LDPC ensemble has threshold ϵ_{TEP} and a critical point at τ' . Assume now a slight deviation of the erasure probability $\epsilon = \epsilon_{\text{TEP}} + \Delta \epsilon$. According to (89), the average fraction of degree-one check nodes has the following Taylor expansion:

$$\begin{aligned} r_1(\tau', n, \epsilon) &= r_1(\tau', n, \epsilon_{\text{TEP}}) + \left. \frac{\partial r_1(\tau, n, \epsilon)}{\partial \epsilon} \right|_{\substack{\tau=\tau' \\ \epsilon=\epsilon_{\text{TEP}}}} \Delta \epsilon \\ &= \gamma_{\text{TEP}} n^{-1} + \left. \frac{\partial r_1(\tau, n, \epsilon)}{\partial \epsilon} \right|_{\substack{\tau=\tau^* \\ \epsilon=\epsilon_{\text{TEP}}}} \Delta \epsilon. \end{aligned} \quad (94)$$

We assume that decoding trajectories are Gaussian distributed around the mean in (94) with a variance denoted by $\delta_{r_1, r_1}^{\text{TEP}}(\tau')/n$. To estimate the TEP error probability, we consider that the TEP decoder will succeed with high probability as long as the fraction of degree-one check nodes at τ' is positive. Therefore,

$$\begin{aligned} \mathbb{E}_{\text{LDPC}[\lambda(x), \rho(x), n]} [P_W^{\text{TEP}}(\mathcal{C}, \epsilon)] &\approx 1 - \mathcal{Q}\left(-\left(\frac{\left. \frac{\partial r_1(\tau, n, \epsilon)}{\partial \epsilon} \right|_{\substack{\tau=\tau' \\ \epsilon=\epsilon_{\text{TEP}}}} \Delta \epsilon + \gamma_{\text{TEP}} n^{-1}}{\sqrt{\delta_{r_1, r_1}^{\text{TEP}}(\tau')/n}}\right)\right) \\ &= \mathcal{Q}\left(\frac{\sqrt{n}(\epsilon_{\text{TEP}} - \epsilon)}{\alpha_{\text{TEP}}} + \frac{\gamma_{\text{TEP}}}{\sqrt{n} \delta_{r_1, r_1}^{\text{TEP}}(\tau')}\right), \end{aligned} \quad (95)$$

where $P_W^{\text{TEP}}(\mathcal{C}, \epsilon)$ is the TEP block error rate for the code $\mathcal{C} \in \text{LDPC}[\lambda(x), \rho(x), n]$ and

$$\alpha_{\text{TEP}} = \sqrt{\delta_{r_1, r_1}^{\text{TEP}}(\tau)} \left(\left. \frac{\partial r_1(\tau, n, \epsilon)}{\partial \epsilon} \right) \right|_{\substack{\tau=\tau' \\ \epsilon=\epsilon_{\text{TEP}}}}^{-1}. \quad (96)$$

The analytical computation of the normalized variance $\delta_{r_1, r_1}^{\text{TEP}}(\tau')/n$ at the critical point requires to solve the covariance graph evolution equations for the TEP and each particular ensemble [18], [20]. Nevertheless, a first approach to this parameter is given by the BP variance at the corresponding critical point, i.e. $\delta_{r_1, r_1}^{\text{BP}}(\tau^*)$. This approximation lies in the fact that the variance of the trajectories essentially comes from the channel dispersion [49] and from the ensemble [18]. Therefore, we do not expect a significant mismatch between $\delta_{r_1, r_1}^{\text{TEP}}(\tau')$ and $\delta_{r_1, r_1}^{\text{BP}}(\tau)$. Besides, for $n \rightarrow \infty$, both the TEP and BP converge to the same performance, so we set $\alpha_{\text{TEP}} = \alpha_{BP}$. In any case, when assuming these values for the TEP parameters, we are overestimating the TEP performance because the better the decoder is, the less variance we expect among different trajectories.

Therefore, provided the TEP SL in (95), to obtain the scaling parameters for a given LDPC ensembles we just have to compute γ_{TEP} using the TEP decoder expected evolution equations provided in Section IV and compute $\delta_{r_1, r_1}^{\text{TEP}}(\tau')$ and α_{TEP} using the analytical expression for the corresponding parameters under BP decoding [18], [20], [50], [51].

Let us include a couple of examples. In Fig. 10 (a), we compare the SL solution in (95) in dashed lines with real

performance data obtained through simulation in solid lines for the regular (3, 6) LDPC ensemble for code lengths $n = 2^{10}$ (∇), $n = 2^{11}$ (\diamond) and $n = 2^{12}$ ($+$). As shown in [29], for these code lengths the TEP significantly improves the BP solution. The match between dashed and solid lines is quite good, proving the accuracy of the model for the TEP performance and the parameter estimation proposed. Due to the parameter overestimation when assuming the BP values for $\delta_{r_1, r_1}^{\text{TEP}}(\tau')/n$ and α_{TEP} , we slightly overestimate the TEP error probability. The overestimation is also caused because in our estimate of $r_1(\tau, n, \epsilon)$ under TEP decoding we do not take into account scenarios where two variables that share a degree-two check node, also share more than one additional check node. For the code lengths considered, these scenarios can be eventually found and the mean can be slightly higher.

In Fig. 10 (b), we include with similar conclusions the results for the irregular code defined in (83) and (84). In all cases, the real error curves have been averaged throughout one hundred code samples chosen to present large enough minimum distance so that the error floor is far below 10^{-4} .

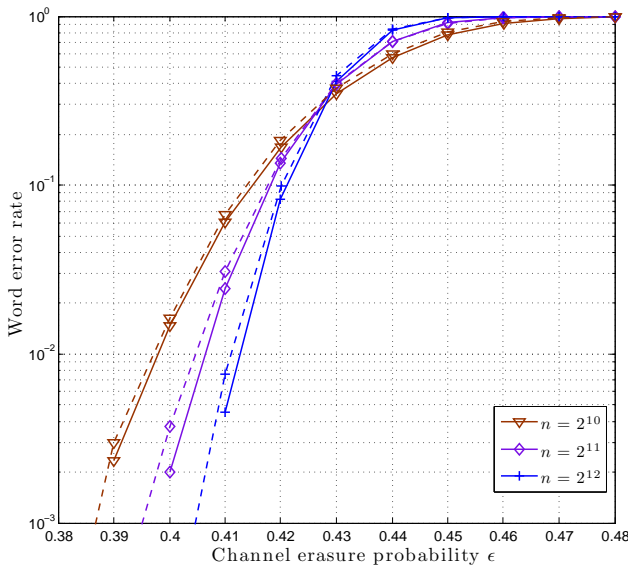
VI. CONCLUSIONS

In this paper, we present the expectation propagation algorithm to address the LDPC decoding process over any DMC. The posterior distribution of the variables is approximated with a Markov-tree probability distribution, over which the marginal estimate can be efficiently performed. By construction, the solution improves the BP estimate. For the binary erasure channel, we show that the tree-EP algorithm reduces to a peeling-type algorithm, i.e. the TEP decoder, that outperforms the BP solution by additionally processing degree-two check nodes and not only degree-one check nodes. The TEP decoder improvement in performance is significant for

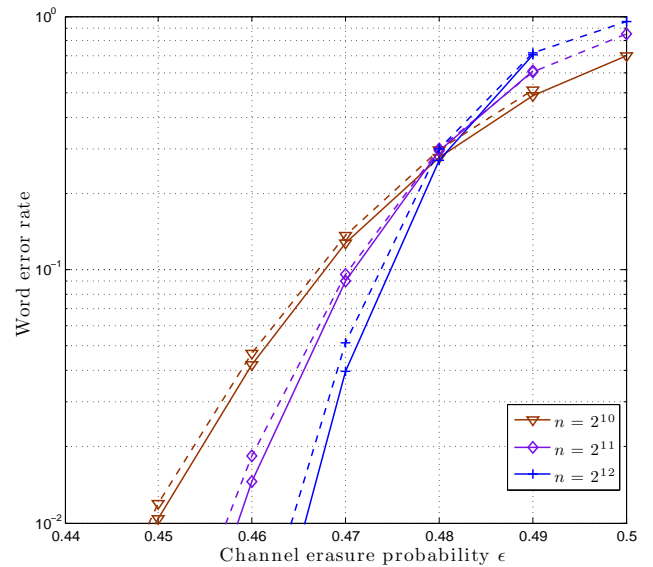
practical finite-length LDPC codes. We have proved that the complexity of this additional step is bounded even in the limiting case and therefore, the TEP complexity is of the same order than the BP algorithm. In the asymptotic regime, we show the conditions that have to be achieved in order to improve the BP threshold. A method to predict the graph evolution under TEP decoding is proposed for finite-length LDPC ensembles. Using this model, we explain the TEP decoder improvement and we have derived an scaling law to predict the performance. The analysis proposed in this paper is a guideline to construct efficient implementations of the Tree-EP algorithm to outperform the BP solution in other channels like the binary symmetry channel and the gaussian-noise channel.

REFERENCES

- [1] R. G. Gallager, *Low Density Parity Check Codes*. MIT Press, 1963.
- [2] J. Pearl, *Probabilistic reasoning in intelligent systems: networks of plausible Inference*. Morgan Kaufmann, 1988.
- [3] D. J. C. MacKay and R. M. Neal, "Near Shannon limit performance of low density parity check codes," *Electronics Letters*, vol. 32, pp. 1645–1646, 1996.
- [4] D. J. C. MacKay, "Good error-correcting codes based on very sparse matrices," *IEEE Transactions on Information Theory*, vol. 45, no. 2, pp. 399–431, 1999.
- [5] H. A. Loeliger, "An introduction to factor graphs," *IEEE Signal Processing Magazine*, vol. 21, no. 1, pp. 28–41, Feb. 2004.
- [6] F. R. Kschischang, B. I. Frey, and H. A. Loeliger, "Factor graphs and the sum-product algorithm," *IEEE Transactions on Information Theory*, vol. 47, no. 2, pp. 498–519, Feb. 2001.
- [7] N. Wiberg, "Codes and decoding on general graphs," Ph.D. dissertation, Department of Electrical Engineering Linköping University, 1996.
- [8] S. M. Aji and R. J. McEliece, "The generalized distributive law," *IEEE Transactions on Information Theory*, vol. 46, no. 2, pp. 325–343, Mar. 2000.
- [9] R. M. Tanner, "A recursive approach to low complexity codes," *IEEE Transactions on Information Theory*, vol. 27, no. 5, pp. 533–547, Sept. 1981.



(a)



(b)

Fig. 10. In (a), we compare the TEP performance for the regular (3, 6) ensemble (solid lines) with the approximation in (95) (dashed lines), using the approximation $\alpha_{\text{TEP}} \approx 0.56036$, $\delta_{r_1, r_1}^{\text{TEP}}(\tau^*) \approx 0.0526$ and $\gamma_{\text{TEP}} \approx 0.3194$. We plot the results for code lengths of $n = 2^{10}$ (∇), $n = 2^{11}$ (\diamond) and $n = 2^{12}$ ($+$). In (b), we reproduce the same figure for the irregular LDPC code defined in (83) and (84). The SL parameters are $\alpha_{\text{TEP}} \approx 0.6887$, $\delta_{r_1, r_1}^{\text{TEP}}(\tau^*) \approx 0.0593$ and $\gamma_{\text{TEP}} \approx 0.2925$.

- [10] T. Richardson and R. Urbanke, "The capacity of low-density parity check codes under message-passing decoding," *IEEE Transactions on Information Theory*, vol. 47, no. 2, pp. 599–618, Feb. 2001.
- [11] —, *Modern Coding Theory*. Cambridge University Press, Mar. 2008.
- [12] C. Measson, A. Montanari, and R. Urbanke, "Maxwell construction: the hidden bridge between iterative and maximum a posteriori decoding," *IEEE Transactions on Information Theory*, vol. 54, no. 12, pp. 5277–5307, Dec. 2008.
- [13] C. Di, D. Proietti, T. Richardson, E. Telatar, and R. Urbanke, "Finite length analysis of low-density parity-check codes on the binary erasure channel," *IEEE Transactions on Information Theory*, vol. 48, no. 6, pp. 1570–1579, Jun. 2002.
- [14] P. Oswald and A. Shokrollahi, "Capacity-achieving sequences for the erasure channel," *IEEE Transactions on Information Theory*, vol. 48, no. 12, pp. 3017–3028, Dec. 2002.
- [15] M. Luby, M. Mitzenmacher, A. Shokrollahi, D. Spielman, and V. Stemann, "Efficient erasure correcting codes," *IEEE Transactions on Information Theory*, vol. 47, no. 2, pp. 569–584, Feb. 2001.
- [16] A. E. Ashikhmin, G. Kramer, and S. ten Brink, "Extrinsic information transfer functions: model and erasure channel properties," *IEEE Transactions on Information Theory*, vol. 50, no. 11, pp. 2657–2673, Nov. 2004.
- [17] J. Zhang and A. Orlitsky, "Finite-length analysis of LDPC codes with large left degrees," in *2002 IEEE International Symposium on Information Theory, ISIT*, 2002.
- [18] A. Amraoui, A. Montanari, T. Richardson, and R. Urbanke, "Finite-length scaling for iteratively decoded LDPC ensembles," *IEEE Transactions on Information Theory*, vol. 55, no. 2, pp. 473–498, 2009.
- [19] A. Amraoui, R. Urbanke, and A. Montanari, "Finite-length scaling of irregular LDPC code ensembles," in *2005 IEEE Information Theory Workshop*, Aug. 2005.
- [20] N. Takayuki, K. Kasai, and S. Kohichi, "Analytical solution of covariance evolution for irregular LDPC codes," *e-prints*, Nov. 2010. [Online]. Available: <http://adsabs.harvard.edu/abs/2010arXiv1011.1701T>
- [21] C. Di, T. Richardson, and R. Urbanke, "Weight distribution of low-density parity-check codes," *IEEE Transactions on Information Theory*, vol. 52, no. 11, pp. 4839–4855, 2006.
- [22] A. Orlitsky, K. Viswanathan, J. Zhang, and S. Member, "Stopping set distribution of LDPC code ensembles," *IEEE Transactions Information Theory*, vol. 51, pp. 929–953, 2005.
- [23] T. P. Minka, "Expectation Propagation for approximate Bayesian inference," in *Proceedings of the 17th Conference in Uncertainty in Artificial Intelligence (UAI 2001)*. Morgan Kaufmann Publishers Inc., 2001, pp. 362–369.
- [24] T. M. Cover and J. A. Thomas, *Elements of information theory*. New York, NY, USA: Wiley-Interscience, 2005.
- [25] J. S. Yedidia, W. T. Freeman, and Y. Weiss, "Generalized belief propagation," in *Proceedings of the Neural Information Processing Systems Conference, (NIPS)*, vol. 13, 2001, pp. 689–695.
- [26] T. Minka and Y. Qi, "Tree-structured approximations by expectation propagation," in *Proceedings of the Neural Information Processing Systems Conference, (NIPS)*, 2003.
- [27] Z. Ghahramani and M. I. Jordan, "Factorial hidden markov models," *Machine Learning*, vol. 29, pp. 245–273, Nov. 1997.
- [28] P. M. Olmos, J. J. Murillo-Fuentes, and F. Pérez-Cruz, "Tree-structure expectation propagation for decoding LDPC codes over binary erasure channels," in *2010 IEEE International Symposium on Information Theory, ISIT, Austin, Texas*, 2010.
- [29] P. Olmos, J. Murillo-Fuentes, and F. Pérez-Cruz, "Tree-structured expectation propagation for decoding finite-length LDPC codes," *IEEE Communications Letters*, vol. 15, no. 2, pp. 235–237, Feb. 2011.
- [30] H. Pishro-Nik and F. Fekri, "On decoding of low-density parity-check codes over the binary erasure channel," *IEEE Transactions on Information Theory*, vol. 50, no. 3, pp. 439–454, Mar. 2004.
- [31] D. Burshtein and G. Miller, "Efficient maximum-likelihood decoding of ldpc codes over the binary erasure channel," *IEEE Transactions on Information Theory*, vol. 50, no. 11, pp. 2837–2844, nov. 2004.
- [32] G. Liva, B. Matuz, E. Paolini, and M. Chiani, "Pivoting Algorithms for Maximum Likelihood Decoding of LDPC Codes over Erasure Channels," in *IEEE Global Telecommunications Conference, 2009. GLOBECOM 2009*, dec. 2009, pp. 1–6.
- [33] S. Kim, S. Lee, and S.-Y. Chung, "An efficient algorithm for ML decoding of raptor codes over the binary erasure channel," *IEEE Communications Letters*, vol. 12, no. 8, pp. 578–580, aug. 2008.
- [34] T. K. Moon, *Error Correction Coding: Mathematical Methods and Algorithms*. Wiley-Interscience, 2005.
- [35] H. Loeliger, "An introduction to factor graphs," *IEEE Signal Processing Magazine*, pp. 28–41, Jan. 2004.
- [36] T. Etzion, A. Trachtenberg, and A. Vardy, "Which codes have cycle-free tanner graphs?" *IEEE Transactions on Information Theory*, vol. 45, no. 6, pp. 2173–2181, sep 1999.
- [37] M. J. Wainwright and M. I. Jordan, *Graphical Models, Exponential Families, and Variational Inference*. Foundations and Trends in Machine Learning, 2008.
- [38] C. M. Bishop, *Pattern Recognition and Machine Learning (Information Science and Statistics)*. Secaucus, NJ, USA: Springer-Verlag New York, Inc., 2006.
- [39] T. P. Minka, "A family of algorithms for approximate bayesian inference," Ph.D. dissertation, Massachusetts Institute of Technology, 2001.
- [40] S. L. Lauritzen, "Propagation of probabilities, means and variances in mixed graphical association models," *Journal of the American Statistical Association*, vol. 87, no. 420, pp. 1098–1108, 1992.
- [41] X. Boyen and D. Koller, "Tractable Inference for Complex Stochastic Processes," in *Uncertainty in Artificial Intelligence*. Morgan Kaufmann, 1998, pp. 33–42.
- [42] A. Becker, R. Bar-Yehuda, and D. Geiger, "Randomized algorithms for the loop cutset problem," *Journal of Artificial Intelligence Research*, vol. 12, no. 1, pp. 219–234, 2000.
- [43] M. Luby, M. Mitzenmacher, A. Shokrollahi, D. Spielman, and V. Stemann, "Practical loss-resilient codes," in *Proceedings of the 29th annual ACM Symposium on Theory of Computing*, 1997, pp. 150–159.
- [44] A. Abbasfar, D. Divsalar, and K. Yao, "Accumulate-Repeat-Accumulate Codes," *IEEE Transactions on Communications*, vol. 55, no. 4, pp. 692–702, april 2007.
- [45] H. Pfister and I. Sason, "Accumulate-repeat-accumulate codes: Capacity-achieving ensembles of systematic codes for the erasure channel with bounded complexity," *IEEE Transactions on Information Theory*, vol. 53, no. 6, pp. 2088–2115, june 2007.
- [46] H. Pfister, "Finite-length analysis of a capacity-achieving ensemble for the binary erasure channel," in *IEEE Information Theory Workshop, 2005*, sept. 2005.
- [47] N. C. Wormald, "Differential equations for random processes and random graphs," *Annals of Applied Probability*, vol. 5, no. 4, pp. 1217–1235, 1995.
- [48] M. Mzard and A. Montanari, *Information, Physics, and Computation*, 1st ed. Oxford University Press, 2009.
- [49] Y. Polyanskiy, H. Poor, and S. Verdú, "Channel coding rate in the finite blocklength regime," *IEEE Transactions on Information Theory*, vol. 56, no. 5, pp. 2307–2359, may 2010.
- [50] J. Ezri, A. Montanari, and R. Urbanke, "A generalization of the finite-length scaling approach beyond the BEC," in *2007 IEEE International Symposium on Information Theory, ISIT*, june 2007, pp. 1011–1015.
- [51] J. Ezri, A. Montanari, S. Oh, and R. Urbanke, "The slope scaling parameter for general channels, decoders, and ensembles," in *2008 IEEE International Symposium on Information Theory, ISIT*, jul. 2008, pp. 1443–1447.
- [52] A. Papoulis, *Probability, Random Variables, and Stochastic Processes*, 4th ed. McGraw-hill, 2002.
- [53] B. Bollobas, *Random Graphs*, W. Fulton, A. Katok, F. Kirwan, P. Sarnak, B. Simon, and B. Totaro, Eds. Cambridge University Press, 2001.

APPENDIX A

TEP SOLUTION AND PROCESSING ORDER

We prove that the TEP decoder solution is independent of the processing order, i.e., the order in which check nodes of degree-one and two are removed. Given the parity check matrix of a linear block code \mathbf{H} , we first show that any operation of the TEP decoder has an associated linear operator over \mathbf{H} . Finally, we prove that these operations commute, proving the independence on the processing order.

Consider the $k \times n$ parity check matrix of the code, \mathbf{H} . The TEP algorithm is initialized by removing from the graph all the known variables. The removal of any of these variables from the graph is equivalent to apply a binary linear transformation over the matrix \mathbf{H} to get a new one, $\hat{\mathbf{H}}$, where the variable V_s is completely disconnected, i.e.

$$\hat{\mathbf{H}} = \mathbf{H}\mathbf{A}_s, \quad (97)$$

where \mathbf{A}_s is an n -dimensional identity matrix where the s -th element is zero. It is straightforward to show that the removal of a variable connected to a check node of degree one is performed by applying a linear transform similar to (97).

On the other hand, to remove a check node of degree two from \mathbf{H} , e.g., P_j connected to variables V_o and V_r , the resulting matrix, $\hat{\mathbf{H}}$, is obtained as follows:

$$\hat{\mathbf{H}} = \mathbf{H}\mathbf{B}_{o,r}, \quad (98)$$

$$\mathbf{B}_{o,r} = \mathbf{A}_o + \mathbf{Z}_{o,r}, \quad (99)$$

where $o \neq r$ and $\mathbf{Z}_{o,r}$ is an $n \times n$ matrix with all zeros except $(\mathbf{Z}_{o,r})_{(o,r)} = 1$. We have assumed that variable V_o has been removed and V_r inherits its connections. The symmetric transformation, i.e. remove V_r instead of V_o , is performed by applying the $\mathbf{B}_{r,o}$ operator. Since the final result is one variable with all connections, $\mathbf{B}_{r,o}$ is equivalent to $\mathbf{B}_{o,r}$. With no loss of generality we may assume that the variable on the left in the Tanner graph, or the one in the leftmost column in the parity check matrix, is the removed one.

When applying \mathbf{A}_s after a sequence of operations (transformations), variable s must be connected to a one degree check node. If it was not in the original graph, in \mathbf{H} , some operations are needed first. Similarly, for $\mathbf{B}_{o,r}$ we need variables o and r to share a degree-two check node. Therefore, no any sequence of operations is valid. We study the commutativity by dividing the problem in two scenarios. In the first one, we study the commutativity of two valid sequences for which, if two processed check nodes shared a variable, then they are placed in the same order in both sequences. Then, we investigate if the order of these pairs of check nodes can be reverse and if it affects the final solution.

In the first scenario, we have two valid sequences of operations with the same set of operations but in different ordering. If we prove that the operations commute, we may reorder the operations in the second sequence, denoted hereafter as II , as in the first one, denoted by I , by commuting the matrices. From left to right, i.e. backwards, for every operation in sequence I , we just look for it in sequence II and commute it forward or backwards to place it in the same position as in sequence I . Particularly, we have to show the following:

Suppose we have two valid sequences of operations with the same set of operations but in different ordering. If we prove that the operations commute, we may reorder the operations in the second sequence, denoted hereafter as II , as in the first one, denoted by I , by commuting the matrices. From left to right, i.e. backward, for every operation in sequence I , we just look for it in sequence II and commute it forward or backwards to place it in the same position as in sequence I . Particularly, we have to show the following:

- 1) \mathbf{A}_s and \mathbf{A}_p commute for all s, p ,
- 2) $\mathbf{B}_{o,r}$ and $\mathbf{B}_{v,z}$ commute for all possible pairs $\{o, r\}$ and $\{v, z\}$ for $o \neq r$ and $v \neq z$,
- 3) \mathbf{A}_s and $\mathbf{B}_{o,r}$ commute for all the possible triples $\{s, o, r\}$ for $o \neq r$,

where s, o, r, v and z belong to $\{1, \dots, n\}$. The first case is straightforward since diagonal matrices always commute.

With respect to the other two cases, by (99), we can write

$$\mathbf{B}_{o,r}\mathbf{B}_{v,z} = \mathbf{A}_o\mathbf{A}_v + \mathbf{A}_o\mathbf{Z}_{v,z} + \mathbf{Z}_{o,r}\mathbf{A}_v + \mathbf{Z}_{o,r}\mathbf{Z}_{v,z}, \quad (100)$$

$$\mathbf{B}_{v,z}\mathbf{B}_{o,r} = \mathbf{A}_v\mathbf{A}_o + \mathbf{A}_v\mathbf{Z}_{o,r} + \mathbf{Z}_{v,z}\mathbf{A}_o + \mathbf{Z}_{v,z}\mathbf{Z}_{o,r}. \quad (101)$$

Note that, to prove both 2) and 3), we have to show that the matrices \mathbf{A}_o and $\mathbf{Z}_{v,z}$ commute for all the possible triples $\{o, v, z\}$ and that $\mathbf{Z}_{o,r}$ and $\mathbf{Z}_{v,z}$ commute as well. Regarding the first case, we have

$$\mathbf{Z}_{v,z}\mathbf{A}_o = \mathbf{Z}_{v,z} \quad z \neq o \quad (102)$$

$$\mathbf{Z}_{v,z}\mathbf{A}_o = \mathbf{0}_{n \times n} \quad z = o, \quad (103)$$

where $\mathbf{0}_{n \times n}$ is the n -square zero matrix. On the other hand,

$$\mathbf{A}_o\mathbf{Z}_{v,z} = \mathbf{Z}_{v,z} \quad o \neq v \quad (104)$$

$$\mathbf{A}_o\mathbf{Z}_{v,z} = \mathbf{0}_{n \times n} \quad o = v, \quad (105)$$

and, hence, we conclude that \mathbf{A}_o and $\mathbf{Z}_{v,z}$ commute as long as $o \neq z$ and $o \neq v$. However, note that $\mathbf{A}_o\mathbf{Z}_{v,o}$ and $\mathbf{A}_v\mathbf{Z}_{v,z}$ are not valid sequences of transformations. Once variable o or v is removed, the check node of degree two, which is connected to is reduced to degree one. Therefore, sequence I will not contain an operation \mathbf{A}_o at the left of operator $\mathbf{Z}_{v,o}$. Similarly, \mathbf{A}_v will not be at the left of $\mathbf{Z}_{v,z}$.

Finally, to conclude the proof, we have to show that the matrices $\mathbf{Z}_{o,r}$ and $\mathbf{Z}_{v,z}$ commute. It is easy to check that

$$\mathbf{Z}_{o,r}\mathbf{Z}_{v,z} = \mathbf{Z}_{v,z}\mathbf{Z}_{o,r} \quad (106)$$

for $o \neq z$ and $v \neq r$. Similarly to what is observed in (102)-(105), Those cases for which the product $\mathbf{Z}_{o,r}\mathbf{Z}_{v,z}$ does not commute, i.e. $o = z$ or $v = w$, are not valid. Once we have removed one variable, we cannot remove it again. By commutativity we conclude that when two check nodes that do not share any variable are removed the TEP yields the same result, regardless of the processing order. Hence, we have proven that any two valid sequences in the first scenario commute.

In the light of the demonstration of commutativity, we still have to investigate whether the processing of two check nodes that share one variable node can be reversed or not. We observe that we have the product

$$\mathbf{Z}_{o,s}\mathbf{A}_s \quad (107)$$

whenever the operators $\mathbf{B}_{o,r}\mathbf{A}_s$ are applied to \mathbf{H} , as illustrated in Fig. 11, meaning that variable V_o is first removed and then we multiply by \mathbf{A}_s to remove V_s . Therefore, $\mathbf{B}_{o,s}\mathbf{A}_s = \mathbf{A}_o\mathbf{A}_s$. We have equivalence between two valid sequences not only if they have the same set of operations, but also if one have any operation \mathbf{A}_o at the left of \mathbf{A}_s while the other has operation $\mathbf{B}_{o,r}$ preceding \mathbf{A}_s . Similarly, an operation $\mathbf{B}_{p,w}$ at the left of $\mathbf{B}_{o,w}$ in one sequence, can be found as an operation $\mathbf{B}_{o,p}$ preceding $\mathbf{B}_{p,w}$ in the other. We conclude that when two check nodes that share some variable are removed they yield the same result, regardless of the processing order. Also, the processing order may lead to different sequences of operations. In the case of a check node of degree one and another of degree two, all variables are revealed. If both of them are of degree two, the only difference is the final variable remaining.

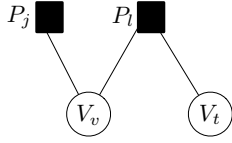


Fig. 11. The TEP decoder can process the graph in (a) by either first removing P_j and V_v and then process check node P_l or, indistinctly, remove first P_l and V_t to then process the degree-one check node P_j

APPENDIX B

PROBABILITY OF SHARING TWO CHECK NODES

In this subsection we compute the probability $p_B(t)$ in (58). Recall that it is defined as the probability for scenario \mathcal{S}_2^B , where two variables share a check node of degree two and, at least, another check node of arbitrary degree, as illustrated in Fig. 4(b). Let $\mathcal{S}_2^{B_m}$ the particular case where both variables share $m+1$ check nodes, one of them at least of degree two. If we compute the probability

$$p(\mathcal{S}_2^{B_m} | \mathcal{S}_2), \quad (108)$$

then the probability $p_B(t)$ is computed by summing over the parameter m :

$$p_B(t) = p(\mathcal{S}_2^B | \mathcal{S}_2) = \sum_m p(\mathcal{S}_2^{B_m} | \mathcal{S}_2). \quad (109)$$

In what follows, we proceed by evaluating the probability of scenarios $\mathcal{S}_2^{B_1}$ and $\mathcal{S}_2^{B_2}$ to finally conclude that

$$p(\mathcal{S}_2^{B_1} | \mathcal{S}_2) \gg p(\mathcal{S}_2^{B_2} | \mathcal{S}_2) \gg p(\mathcal{S}_2^{B_3} | \mathcal{S}_2) \cdots \quad (110)$$

and, for large enough graphs, we have

$$p(\mathcal{S}_2^B | \mathcal{S}_2) = p(\mathcal{S}_2^{B_1} | \mathcal{S}_2) + \mathcal{O}(1/E^2), \quad (111)$$

which means that, in practice, we only have to consider the scenario $\mathcal{S}_2^{B_1}$ to study the TEP decoder for large code lengths.

1) *Probability of scenario $\mathcal{S}_2^{B_1}$* : We first focus on the scenario $\mathcal{S}_2^{B_1}$, illustrated in Fig. 4(b). Our goal is to compute the probability $p(\mathcal{S}_2^{B_1, j} | \mathcal{S}_2)$, where $\mathcal{S}_2^{B_1, j}$ corresponds to the case where V_p and V_q share just a check node of degree two and a check node of degree j . Then, the probability (111) is computed by marginalizing over the degree j :

$$p(\mathcal{S}_2^{B_1} | \mathcal{S}_2) = \sum_{j=1}^{j_{\max}} p(\mathcal{S}_2^{B_1, j} | \mathcal{S}_2). \quad (113)$$

If $d_{V_o}(j)$ denotes the number of edges connected to V_o that have right degree j , we propose to obtain the probability $p(\mathcal{S}_2^{B_1, j} | \mathcal{S}_2)$ by marginalizing over the following probability function:

$$p(\mathcal{S}_2^{B_1, j}, d_{V_o}, d_{V_r}, d_{V_o}(j) = \theta, d_{V_r}(j) = \vartheta | \mathcal{S}_2), \quad (114)$$

for $\theta \in \{0, \dots, d_{V_o} - 1\}$, $\vartheta \in \{0, \dots, d_{V_r} - 1\}$. The mass probability function in (114) represents the probability that V_o and V_r share another check node of degree j , the degree of V_o and V_r is, respectively, d_{V_o} and d_{V_r} , V_o has θ edges of right degree j and V_r has ϑ edges of right degree j . The

probability density function in (114) can be rewritten applying the properties of conditional probability:

$$\begin{aligned} p(\mathcal{S}_2^{B_1, j}, d_{V_o}, d_{V_r}, d_{V_o}(j) = \theta, d_{V_r}(j) = \vartheta | \mathcal{S}_2) \\ = p(\mathcal{S}_2^{B_1, j} | d_{V_o}(j) = \theta, d_{V_r}(j) = \vartheta, d_{V_o}, d_{V_r}, \mathcal{S}_2) \\ \cdot p(d_{V_o}(j) = \theta, d_{V_r}(j) = \vartheta | d_{V_o}, d_{V_r}, \mathcal{S}_2) \\ \cdot p(d_{V_o}, d_{V_r} | \mathcal{S}_2). \end{aligned} \quad (115)$$

The degrees of two given nodes in the graph are (asymptotically) pairwise independent [48] and, hence, for sufficiently large graphs we can assume

$$p(d_{V_o}, d_{V_r} | \mathcal{S}_2) = \frac{l_{d_{V_o}}(t)}{e(t)} \frac{l_{d_{V_r}}(t)}{e(t)} + \mathcal{O}(E^{-1}), \quad (116)$$

for $d_{V_o}, d_{V_r} \in \{2, \dots, E\}$. Each edge connected to a variable node has right degree j with probability $r_j(t)/e(t)$. The number of edges connected to either V_o or V_r with right degree j are asymptotically distributed according to binomial distributions $B(\theta, d_{V_o} - 1, r_j(t)/e(t))$ and $B(\vartheta, d_{V_r} - 1, r_j(t)/e(t))$ respectively, where $B(x, N, P)$ denotes a binomial distribution over $x \in \mathbb{N}$ with parameters N and P [52]. Note that we subtract 1 to d_{V_o} and d_{V_r} since we know that one edge is connected to a check node of degree two. Therefore, the second term in (115) is

$$\begin{aligned} p(d_{V_o}(j) = \theta, d_{V_r}(j) = \vartheta | d_{V_o}, d_{V_r}, \mathcal{S}_2) = \\ = B\left(\theta, d_{V_o} - 1, \frac{r_j(t)}{e(t)}\right) \cdot B\left(\vartheta, d_{V_r} - 1, \frac{r_j(t)}{e(t)}\right) + \mathcal{O}(E^{-1}). \end{aligned} \quad (117)$$

Finally, we have to compute the first term in (115), i.e., the probability that variables V_o and V_r share a check node of degree j when the variables have, respectively, θ and ϑ edges with right degree j . Note first that the graph has $r_j(t)E$ edges with right degree j . Let us assume that the edges of one of the variables, V_o for example, are fixed and that the edges of V_r are now randomly set.

If the graph is large enough, with probability

$$\frac{\theta(j-1)}{Er_j(t)}, \quad (118)$$

each edge of V_r shares a check node of degree j with an edge of V_o . For large graphs, the number of checks shared between both variables is asymptotically described by a binomial distribution $B(\vartheta, \theta(j-1)/Er_j(t))$. The probability that they share at least one check node of degree j in (115) yields

$$\begin{aligned} p(\mathcal{S}_2^{B_1, j} | d_{V_o}(j) = \theta, d_{V_r}(j) = \vartheta, d_{V_o}, d_{V_r}, \mathcal{S}_2) \\ = \vartheta \frac{\theta(j-1)}{Er_j(t)} \left(1 - \frac{\theta(j-1)}{Er_j(t)}\right)^{\vartheta-1} \\ \approx \frac{\vartheta\theta(j-1)}{Er_j(t)} + \mathcal{O}(E^{-2}). \end{aligned} \quad (119)$$

We have already computed all the factors in the joint mass function in (115). In (112), we marginalize over d_{V_o}, d_{V_r}, θ and ϑ to obtain $p(\mathcal{S}_2^{B_1, j} | \mathcal{S}_2)$:

$$p(\mathcal{S}_2^{B_1, j} | \mathcal{S}_2) = \frac{(j-1)r_j(t)}{Ee^2(t)} (l_{\text{avg}}(t) - 1)^2. \quad (120)$$

Finally, the probability of scenario $\mathcal{S}_2^{B_1}$ is computed by marginalizing over the degree j as follows

$$p(\mathcal{S}_2^{B_1}|\mathcal{S}_2) = \sum_{j=1}^{j_{\max}} p(\mathcal{S}_2^{B_1,j}|\mathcal{S}_2) = \frac{(l_{\text{avg}}(t) - 1)^2 (r_{\text{avg}}(t) - 1)}{Ee(t)}. \quad (121)$$

As expected, the probability of two variables sharing a check node in a random graph (aside from the check node of degree two that we know they are sharing) is $\mathcal{O}(E^{-1}e(t)^{-1})$, i.e., inverse to the total number of edges in the graph. This result is consistent with the theory of random graphs [53].

2) *Probability of scenario $\mathcal{S}_2^{B_u}$ for $u > 1$:* A similar analysis can be extended for the case $\mathcal{S}_2^{B_2}$. If we define the subscenario $\mathcal{S}_2^{B_2,j,\ell}$, where both variables share two check nodes of degrees j and ℓ , the probability $p(\mathcal{S}_2^{B_2}|\mathcal{S}_2)$ is obtained by counting over all possible cases:

$$p(\mathcal{S}_2^{B_2}|\mathcal{S}_2) = \sum_{j,\ell} p(\mathcal{S}_2^{B_2,j,\ell}|\mathcal{S}_2). \quad (122)$$

The probability $p(\mathcal{S}_2^{B_2,j,\ell}|\mathcal{S}_2)$ can be obtained with a similar procedure than the one used to compute $p(\mathcal{S}_2^{B_1,j}|\mathcal{S}_2)$. In this case, we marginalize over the joint mass probability function of the degrees of both variables (d_{V_o}, d_{V_r}) the number of edges in each variable with right degree j ($d_{V_o}(j), d_{V_r}(j)$) and the number of edges in each variable with right degree ℓ ($d_{V_o}(\ell), d_{V_r}(\ell)$). Now we factorize the joint mass function applying the conditionality properties, as we did in (115):

$$\begin{aligned} p(\mathcal{S}_2^{B_2,j,\ell}, d_{V_o}, d_{V_r}, d_{V_o}(j), d_{V_r}(j), d_{V_o}(\ell), d_{V_r}(\ell) | \mathcal{S}_2) \\ = p(\mathcal{S}_2^{B_2,j,\ell} | d_{V_o}(\ell), d_{V_r}(\ell), d_{V_o}(j), d_{V_r}(j), d_{V_o}, d_{V_r}, \mathcal{S}_2) \\ \cdot p(d_{V_o}(\ell), d_{V_r}(\ell), d_{V_o}(j), d_{V_r}(j) = \beta | d_{V_o}, d_{V_r}, \mathcal{S}_2) \\ \cdot p(d_{V_o}, d_{V_r} | \mathcal{S}_2), \end{aligned} \quad (123)$$

where the last factor $p(d_{V_o}, d_{V_r} | \mathcal{S}_2)$ does not change with respect to (116) and the second one, similarly to (117), can be expressed as a product of binomial distributions. In the first

term in (123), we have fixed the degrees of V_o and V_r and the number of edges of both variables with right degree j and ℓ . Following the same procedure considered to derive (119), it can be shown that

$$\begin{aligned} p(\mathcal{S}_2^{B_2,j,\ell} | d_{V_o}(\ell), d_{V_r}(\ell), d_{V_o}(j), d_{V_r}(j), d_{V_o}, d_{V_r}, \mathcal{S}_2) \\ = \frac{d_{V_o}(j) d_{V_r}(j) (j-1)}{Er_j(t)} \frac{d_{V_o}(\ell) d_{V_r}(\ell) (\ell-1)}{Er_\ell(t)} \propto E^{-2} \end{aligned} \quad (124)$$

The constant E^{-2} does not depend on the marginalization in (122). Hence,

$$p(\mathcal{S}_2^{B_2}|\mathcal{S}_2) \propto \frac{1}{E^2} \quad (125)$$

and, in general we have:

$$p(\mathcal{S}_2^{B_m}|\mathcal{S}_2) \propto \frac{1}{E^m}, \quad (126)$$

for $m \in \mathbb{N}$. Therefore $p(\mathcal{S}_2^{B_m}|\mathcal{S}_2)$ for $m \geq 2$ are negligible compared to $p(\mathcal{S}_2^{B_1}|\mathcal{S}_2)$ for sufficiently large graphs.

Probability $p_B(t)$ is crucial to evaluate the expected graph evolution under TEP decoding in Section IV. In addition, for asymptotically large graphs, to evaluate how the graph changes in one iteration of the TEP decoder, it is a good approximation to consider that two variables that are sharing a check node of degree two, share at most one extra check node, as illustrated in Fig. 4(b).

APPENDIX C

BOUNDEDNESS ON THE GRAPH DEGREES. PROOF OF LEMMA 2

Consider an LDPC code \mathcal{C} with parity check matrix \mathbf{H} and rate \mathbf{r} . After transmission over the BEC, we initialize the Tanner graph by removing all non-erased variables, see Section III-A. The residual graph is non-empty and it corresponds to a code for which we can compute the rate as follows [11]:

$$\mathbf{r}(t=0, \mathbf{y}) = 1 - \frac{\Lambda_{\text{avg}}(t=0, \mathbf{y}, \mathcal{C})}{\Theta_{\text{avg}}(t=0, \mathbf{y}, \mathcal{C})}. \quad (127)$$

$$\begin{aligned} p(\mathcal{S}_2^{B_1,j}|\mathcal{S}_2) &= \sum_{\substack{d_{V_o}, d_{V_r} \\ \theta, \vartheta}} p(\mathcal{S}_2^{B_1,j}, d_{V_o}, d_{V_r}, d_{V_o}(j) = \theta, d_{V_r}(j) = \vartheta | \mathcal{S}_2) \\ &= \sum_{d_{V_o}, d_{V_r}} \left[\frac{l_{d_{V_o}}(t)}{e(t)} \frac{l_{d_{V_r}}(t)}{e(t)} \sum_{\theta} \binom{d_{V_o}-1}{\theta} \left(\frac{r_j(t)}{e(t)} \right)^{\theta} \left(1 - \frac{r_j(t)}{e(t)} \right)^{d_{V_o}-1-\theta} \right. \\ &\quad \left. \sum_{\vartheta} \binom{d_{V_r}-1}{\vartheta} \left(\frac{r_j(t)}{e(t)} \right)^{\vartheta} \left(1 - \frac{r_j(t)}{e(t)} \right)^{d_{V_r}-1-\vartheta} \frac{\vartheta \theta (j-1)}{Er_j(t)} \right] \\ &= \sum_{d_{V_o}, d_{V_r}} \frac{l_{d_{V_o}}(t)}{e(t)} \frac{l_{d_{V_r}}(t)}{e(t)} \frac{(j-1)}{Er_j(t)} \mathbb{E}[d_{V_o}(j)] \mathbb{E}[d_{V_r}(j)] \\ &= \sum_{d_{V_o}, d_{V_r}} \frac{l_{d_{V_o}}(t)}{e(t)} \frac{l_{d_{V_r}}(t)}{e(t)} \frac{(j-1)}{Er_j(t)} (d_{V_o}-1) (d_{V_r}-1) \left(\frac{r_j(t)}{e(t)} \right)^2 \\ &= \frac{(j-1)r_j(t)}{Ee^2(t)} \left(\sum_{d_{V_o}} \frac{l_{d_{V_o}}(t)}{e(t)} (d_{V_o}-1) \right) \left(\sum_{d_{V_r}} \frac{l_{d_{V_r}}(t)}{e(t)} (d_{V_r}-1) \right) = \frac{(j-1)r_j(t)}{Ee^2(t)} (l_{\text{avg}}(t) - 1)^2. \end{aligned} \quad (112)$$

This graph can be represented by a parity check matrix for which we can equivalently compute the rate in (127) using the ratio between the remaining set columns, call them $N_v(t=0)$ and rows, $N_c(t=0)$ [34]:

$$r(t=0, \mathbf{y}) = 1 - \frac{N_c(t=0)}{N_v(t=0)}. \quad (128)$$

Note that the rate $r(t=0, \mathbf{y})$ is upper-bounded by r and is bigger than $-\infty$. After the initialization process, the number of columns in the original parity matrix can be lower than the number of rows and, hence, the rate can be negative. However, by (127), $r(t=0, \mathbf{y})$ must be finite because $\Lambda_{\text{avg}}(t=0, \mathbf{y}, \mathcal{C})$ and $\Theta_{\text{avg}}(t=0, \mathbf{y}, \mathcal{C})$ are bounded. Besides, by (128) the number of variable nodes and check nodes are of the same order.

The TEP decoder works over the initialized graph by removing one column and one row per iteration. By removing degree-one or degree-two check nodes, we know that the average check degree $\Theta_{\text{avg}}(t, \mathbf{y}, \mathcal{C})$ does not grow. Regarding the variables, $\Lambda_{\text{avg}}(t, \mathbf{y}, \mathcal{C})$ might grow as we remove degree-two check nodes. For an infinitely large code, assume that $\Lambda_{\text{avg}}(t, \mathbf{y}, \mathcal{C}) = \infty$ at some time. By (127), the rate of the code $r(t, \mathbf{y})$ would be $-\infty$. However, by (128), this result implies that $N_v(t) = 0$, in other words, that we have already decoded since there are no variables left in the graph.